ISSN 2096-7071 (Print)
ISSN 2096-3101 (Online)
CN 10-1629/R1

CHINA CDC WEEKLY

Vol. 7 No. 26 Jun. 27, 2025

CCDC weekly

中国疾病预防控制中心周报

Commentary

From Global Consensus to Local Action: China's Strategic Response to Emerging Drug Use Trends 877

Enhanced Genomic Surveillance Is Essential for Effective *Salmonella* Outbreak Response 880

Vital Surveillances

Epidemiological Characteristics and Spatiotemporal Cluster Analysis of Scrub Typhus — China, 2006–2023 882

Preplanned Studies

Niche Analysis of Spatial Distribution and Host Selection of Global *Echinococcus* Species — Worldwide, up to June 30, 2024 889

Drug Resistance of Imported *P. falciparum* and *P. vivax* Isolates — China, 2021–2023 895

Reviews

Tick-Borne Infectious Diseases in Chinese Mainland, 2003–2023 900

ISSN 2096-7071

Editorial Board

Editor-in-Chief Hongbing Shen
Founding Editor George F. Gao
Deputy Editor-in-Chief Liming Li Gabriel M Leung Zijian Feng
Executive Editor Chihong Zhao
Members of the Editorial Board
Rui Chen
Wen Chen
Xi Chen (USA)
Zhuo Chen (USA)
Gangqiang Ding
Xiaoping Dong
Pei Gao
Mengjie Han
Yuantao Hao
Na He
Yuping He
Guoqing Hu
Zhibin Hu
Yueqin Huang
Na Jia
Weihua Jia
Zhongwei Jia
Guangfu Jin
Xi Jin
Biao Kan
Haidong Kan
Ni Li
Qun Li
Ying Li
Zhenjun Li
Min Liu
Qiyong Liu
Xiangfeng Lu
Jun Lyu
Huilai Ma
Jiaqi Ma
Chen Mao
Xiaoping Miao
Ron Moolenaar (USA)
Daxin Ni
An Pan
Lance Rodewald (USA)
William W. Schluter (USA)
Yiming Shao
Xiaoming Shi
Yuelong Shu
RJ Simonds (USA)
Xuemei Su
Chengye Sun
Quanfu Sun
Xin Sun
Feng Tan
Jinling Tang
Huaqing Wang
Hui Wang
Linhong Wang
Tong Wang
Guizhen Wu
Jing Wu
Xifeng Wu (USA)
Yongning Wu
Min Xia
Ningshao Xia
Yankai Xia
Lin Xiao
Hongyan Yao
Zundong Yin
Dianke Yu
Hongjie Yu
Shicheng Yu
Ben Zhang
Jun Zhang
Liubo Zhang
Wenhua Zhao
Yanlin Zhao
Xiaoying Zheng
Maigeng Zhou
Xiaonong Zhou
Guihua Zhuang

Advisory Board

Director of the Advisory Board Jiang Lu
Vice-Director of the Advisory Board Yu Wang Jianjun Liu Jun Yan
Members of the Advisory Board
Chen Fu
Gauden Galea (Malta)
Dongfeng Gu
Qing Gu
Yan Guo
Ailan Li
Jiafa Liu
Peilong Liu
Yuanli Liu
Kai Lu
Roberta Ness (USA)
Guang Ning
Minghui Ren
Chen Wang
Hua Wang
Kean Wang
Xiaoqi Wang
Zijun Wang
Fan Wu
Xianping Wu
Jingjing Xi
Jianguo Xu
Gonghuan Yang
Tilahun Yilma (USA)
Guang Zeng
Xiaopeng Zeng
Yonghui Zhang
Bin Zou

Editorial Office

Directing Editor Chihong Zhao
Managing Editors Yu Chen
Senior Scientific Editors Daxin Ni Ning Wang Wenwu Yin Jianzhong Zhang Qian Zhu
Scientific Editors
Weihong Chen
Tao Jiang
Xudong Li
Nankun Liu
Liwei Shi
Liuying Tang
Meng Wang
Zhihui Wang
Qi Yang
Qing Yue
Lijie Zhang
Ying Zhang

Cover Image: adapted from the United Nations, https://www.unodc.org/unodc/en/drugs/index-new.html.

Commentary

From Global Consensus to Local Action: China's Strategic Response to Emerging Drug Use Trends

Haoliang Cui[1]; Jianyi Zhang[1]; Wenkai Luo[1]; Erri Du[2]; Zhongwei Jia[1,#]

The recognition of drug use as a global challenge requiring coordinated international response began with the first international conference on narcotic drugs held in Shanghai in 1909. Throughout the 20th century, three pivotal United Nations (UN) conventions on drug control (1961, 1971, and 1988) established the legal and institutional framework for a comprehensive multilateral system addressing prevention and enforcement. The creation of the United Nations Office on Drugs and Crime (UNODC) in 1997 further underscored the widespread nature of drug-related challenges confronting societies worldwide (*1*–*2*).

As nations develop more sophisticated approaches to addressing global drug challenges, international surveillance data continue to underscore both the magnitude of the problem and the critical importance of prevention strategies. The global population using drugs has reached 292 million in 2022, representing a 20% increase over the past decade (*3*). Particularly concerning is the finding that cannabis use prevalence among adolescents aged 15–16 years exceeds that of adults worldwide (*3*). It was estimated that 84 million adults aged 15–64 in Europe had used cannabis at least once, including approximately 15.3 million young adults aged 15–34 based on the *European Drug Report 2023*. (*4*). Similarly, in 2022, an estimated 70.3 million individuals aged 12 or older in the United States reported illicit drug use within the past year, with peak prevalence occurring among young adults aged 18 to 25. These statistics demonstrate the urgent need for targeted prevention investments, particularly among youth populations (*5*).

China has actively contributed to and responded to these global drug control initiatives. The Anti-Drug Law of the People's Republic of China (*6*) was enacted in 2007, establishing a comprehensive triadic strategy that encompasses prevention, punishment, and rehabilitation. Following the law's implementation, the number of newly identified drug users increased steadily, reaching its peak in 2015 (Figure 1). However, a series of national initiatives — including the "People's War on Drugs," the "Sword Action" (Liangjian Project), and the deployment of "Skynet" surveillance systems — led to a significant decrease in newly identified drug users. This decline was particularly pronounced during and after the COVID-19 pandemic, when the number of newly found drug users experienced a sharp drop (Figure 1).

The theme of this year's International Day Against Drug Abuse and Illicit Trafficking — "The evidence is clear: invest in prevention, Break the cycle, Stop Organized Crime" (*7*) — underscores the public health nature of the drug problem and emphasizes the critical importance of preventive measures (Figure 2). The evolution of these annual themes reflects a fundamental shift in global attitudes toward drug policy. From 1996 to 2009, themes primarily emphasized the dangers and harmful consequences of drug use. The second stage (2010 to 2015) began treating the drug problem as a public health issue rather than solely a criminal justice matter. Since 2016, the focus has shifted toward prevention, early intervention, and youth-centered strategies, reflecting a more comprehensive and evidence-based approach to drug policy.

Nevertheless, emerging risks continue to challenge existing frameworks. Recent cases of adolescent substance abuse involving compounds not yet under formal regulatory control, such as nitrous oxide and etomidate, have been documented across China (*8*). Since January 2021, Guangzhou in Guangdong Province has implemented targeted enforcement measures against nitrous oxide distribution, resulting in 46 investigated cases by June 2022 (*9*). These novel psychoactive substances present distinct challenges due to their accessibility through online platforms, ambiguous legal classification, and limited public awareness — particularly among adolescents. In response to these evolving threats, the Ministry of Justice issued a national directive in early 2025 emphasizing "intensified drug prevention campaigns targeting adolescents" (*10*). Through strategic investments in early education programs, enhanced

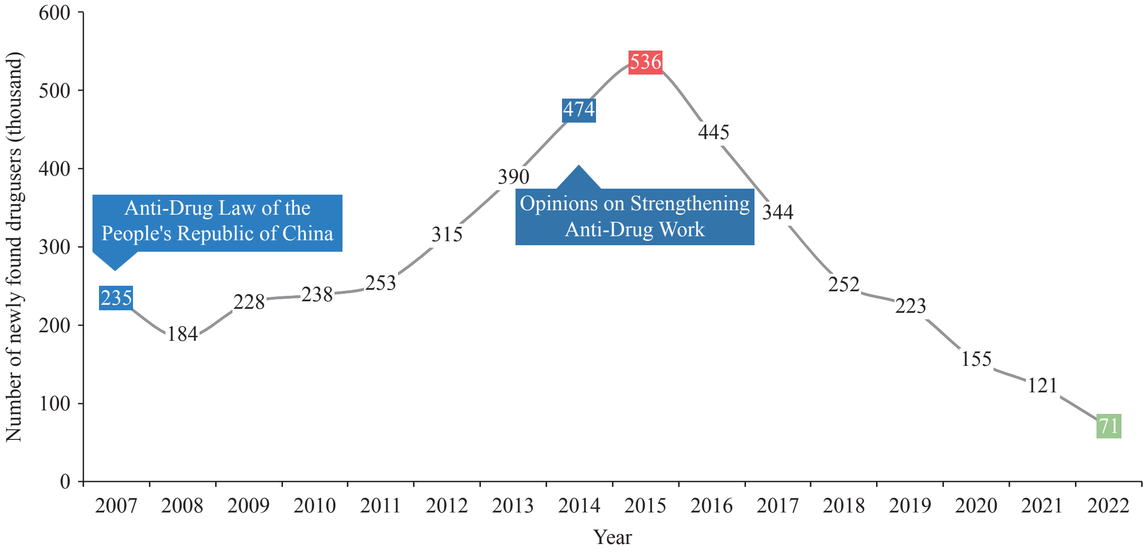

FIGURE 1. Trends in newly identified drug users in China, 2007–2022.
Note: Data from 2007 to 2013 were sourced from the *Drug Abuse Population Estimation in the Key Cities of the Ministry of Public Security*, while data from 2014 to 2022 were obtained from the respective annual editions of the *Drug Situation in China* report.

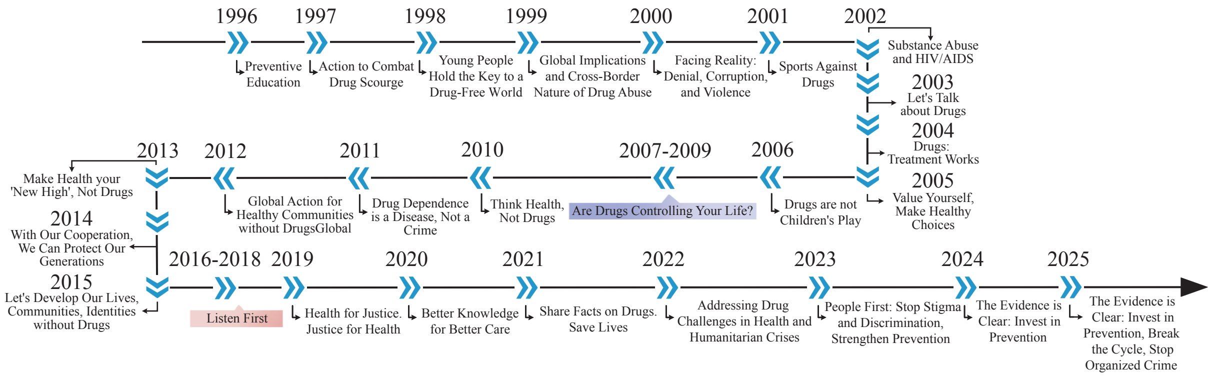

FIGURE 2. Official themes of the International Day Against Drug Abuse and Illicit Trafficking (World Drug Day), 1996–2025.
Note: Data sourced from United Nations publications.

cross-sector collaboration, and implementation of evidence-based policy frameworks, China is proactively adapting its approach to address the dynamic landscape of emerging drug-related risks.

doi: 10.46234/ccdcw2025.145

Corresponding author: Zhongwei Jia, jiazw@bjmu.edu.cn.

---

[1] Department of Global Health, School of Public Health, Peking University, Beijing, China; [2] SILC Business School, Shanghai University, Shanghai, China.

Submitted: June 19, 2025
Accepted: June 23, 2025
Issued: June 27, 2025

REFERENCES

1. United Nations Office on Drugs and Crime (UNODC). About us. 2025. https://www.unodc.org/unodc/en/about-unodc/index.html. [2025-6-17].
2. United Nations Office on Drugs and Crime (UNODC). A century of international drug control. 2009. https://www.unodc.org/documents/data-and-analysis/Studies/100_Years_of_Drug_Control.pdf. [2025-6-17].
3. United Nations Office on Drugs and Crime (UNODC). World drug report 2024 - Key findings and conclusions. 2024. https://www.unodc.org/documents/data-and-analysis/WDR_2024/WDR24_Key_findings_and_conclusions.pdf. [2025-6-22].
4. European Union Drugs Agency. European drug report 2023: Trends and developments. 2023. https://www.emcdda.europa.eu/publications/european-drug-report/2023_en. [2025-6-17].
5. Substance Abuse and Mental Health Services Administration. Key substance use and mental health indicators in the United States: Results from the 2022 national survey on drug use and health. 2023. https://www.cdc.gov/overdose-prevention/media/pdfs/2024/04/SAMHSA-

Key-substance-use-and-mental-health-indicators-2022.pdf. [2025-6-17].

6. National Narcotics Control Commission of China. Anti-drug law of the people's republic of China. 2007. http://www.nncc626.com/2014-05/14/c_126500823.htm. [2025-6-17]. (In Chinese).
7. United Nations Office on Drugs and Crime (UNODC). International day against drug abuse and illicit trafficking. 2025. https://www.unodc.org/unodc/en/drugs/index-new.html. [2025-6-22].
8. Ministry of Public Security of the People's Republic of China. Drug situation in China (2022). 2022. https://www.mps.gov.cn/n6557558/c9085037/content.html. [2025-6-17]. (In Chinese).
9. GDToday. Guangzhou launches special campaign against nitrous oxide, investigates 46 cases. 2022. https://news.southcn.com/node_5439242dce/d29917bd51.shtml. [2025-6-22]. (In Chinese).
10. Ministry of Justice of the People's Republic of China. The justice rehabilitation system launched the 2025 "June 26" international day against drug abuse and illicit trafficking publicity and education campaign. 2025. https://www.moj.gov.cn/pub/sfbgw/zwgkztzl/sfbjdzh/sfbjdzhyw/202506/t20250613_520949.html. [2025-6-17]. (In Chinese).

Commentary

Enhanced Genomic Surveillance Is Essential for Effective *Salmonella* Outbreak Response

Yanan Wang[1,2,#]; Xuebin Xu[3]; Baoli Zhu[4]; George F. Gao[4,5,6]

On May 1, 2025, Gonzalez-Perez and colleagues (*1*) reported a multi-country outbreak caused by *Salmonella enterica* subspecies *enterica* serovar Mbandaka (*S.* Mbandaka) that resulted in over 200 cases across Europe. Finland reported the highest number of cases with 97 infections. Whole genome sequencing (WGS) and comparative genomic analyses revealed that the outbreak strains were genetically linked to previously identified strains in the United Kingdom and to pre-cooked, frozen chicken meat used in ready-to-eat products. Subsequently, on May 5, 2025, the United States of America (USA) Centers for Disease Control and Prevention (CDC) announced a *Salmonella* outbreak associated with backyard poultry (*2*). As of May 19, 2025, this outbreak had expanded to 104 confirmed infections, with at least 33 individuals contracting *Salmonella* following contact with backyard poultry. Tragically, one death has been reported in Illinois. Scientific evidence demonstrates that *S.* Mbandaka isolated from patient samples, and matched the strain found in shipping boxes used to transport poultry from hatcheries to agricultural retail stores. Although confirmed and suspected cases have been reported from 35 states, including Florida, Illinois, Missouri, South Dakota, Utah, and Wisconsin, the actual number of infections likely exceeds reported figures due to underdiagnosis and underreporting. The outbreak's severity prompted the recall of more than 1.7 million eggs due to potential *Salmonella* contamination. Interstate and international transportation of poultry and chicken meat products appear to be facilitating the pathogen's spread across the USA, European countries, and globally. However, our understanding of the genetic characteristics and transmission patterns of *S.* Mbandaka remains limited.

In response to the current outbreak caused by *Salmonella*, which has been listed in the 2024 World Health Organization Bacterial Priority Pathogens List (*3*–*4*) and increasing trends in antimicrobial resistance (AMR) (*5*–*7*), rapid genomic sequencing, together with the timely sharing of data, is vital for assessing the outbreak source tracing, clinical guidance, and formulating effective prevention and control policies (*8*). As of February 15, 2025, 2,814 genomes with clear metadata (including collection date, source, and location of collection information), serovar, and sequence type (ST) were publicly available from the National Center for Biotechnology Information (NCBI). Genomic data submitted to the NCBI were collected from 6 continents, and 66.45% of them were isolated from North America (mainly in the USA), followed by Europe (20.04%) and Asia (8.14%). We identified a clear gap in data from Africa (*n*=13) and Oceania (*n*=48) despite the onward transmission of *S.* Mbandaka in North America and Europe during this time. The majority of genomes were from humans (21.57%), cattle (19.47%), environment (19.40%), chickens (11.05%), food (9.70%), and pigs (6.15%). A total of 18 STs were identified; ST413 (*n*=2,611) was the most dominant, followed by ST1602 (*n*=112). Due to the lack of timely data-sharing and genomic surveillance during this period, the current outbreak caused by *S.* Mbandaka may be underestimated.

Our previous studies demonstrate that *S.* Mbandaka ranks 17th among human infections in China (*7*) and 18th globally among 208,233 *Salmonella* genomes with comprehensive metadata (*6*). Genomic prediction analyses revealed increasing AMR trends in *S.* Mbandaka. We identified 95 acquired antibiotic resistance genes (ARGs) across these genomes. Notably, 4 genomes carried the carbapenem resistance gene $bla_{\mathrm{NDM\text{-}1}}$, while 22 carried the colistin resistance gene *mcr-9*. All 4 strains containing the carbapenem resistance gene $bla_{\mathrm{NDM\text{-}1}}$ were isolated from human patients in China, with 3 recovered from blood samples and 1 were from fecal specimens. Moreover, we detected third-generation cephalosporin resistance genes $bla_{\mathrm{CTX\text{-}M\text{-}65/55/14/1/8}}$ (*n*=16), the fosfomycin resistance gene *fosA7* (*n*=1), and the azithromycin resistance gene *mph(A)* (*n*=22). These comprehensive genomic analyses enlarge our understanding of AMR evolution in *S.* Mbandaka and provide a critical context for interpreting current outbreak patterns.

Salmonella infections represent a significant zoonotic threat, necessitating comprehensive bacterial genomic surveillance that encompasses diverse sources, including humans, animals, food products, plants, and environmental samples. Technological advances in WGS and artificial intelligence (AI) have revolutionized genomic surveillance capabilities, making comprehensive multi-source data collection essential for tracking outbreak origins and monitoring AMR evolution in *S. enterica* (*6*–*9*). A prime example of this approach, is the high-quality, open-access, Chinese local *Salmonella* genome database version 2 (CLSGDBv2, https://nmdc.cn/clsgdbv2) (*10*), which serves as a valuable resource for global genomic surveillance and demonstrates substantial public health impact, having been accessed around 170 thousand times across 6 continents. These developments underscore the urgent need for enhanced genomic sequencing capabilities and improved data-sharing protocols, while simultaneously strengthening public health and clinical laboratory surveillance networks. Consequently, expanding publicly available genomic data for *Salmonella* serovars, particularly Mbandaka, would significantly improve real-time outbreak assessment capabilities, and prioritizing WGS of *Salmonella* strains from food and animal sources in underrepresented geographic regions is essential for comprehensive global surveillance.

Conflicts of interest: No conflicts of interest.

Acknowledgments: The Veterinary Big Data and Bioinformatics Center at Henan Agricultural University, for their technical support and assistance.

Funding: Supported in part by grants from the Project for the Young Scientist of the Joint Funds of Science and Technology Research and Development Plan of Henan Province, China (235200810058), the National Key Research and Development Program of China (2023YFC2307101), and the Young Top-Notch Talents Foundation of Henan Agricultural University (30501278).

doi: 10.46234/ccdcw2025.151

[#] Corresponding author: Yanan Wang, wangyanan1001@henau.edu.cn.

---

[1] International Joint Research Center of National Animal Immunology, College of Veterinary Medicine, Henan Agricultural University, Zhengzhou City, Henan Province, China; [2] Longhu Laboratory of Advanced Immunology, Zhengzhou City, Henan Province, China; [3] Division of Pathogen Testing and Analysis, Shanghai Municipal Center for Disease Control and Prevention, Shanghai, China; [4] CAS Key Laboratory of Pathogen Microbiology and Immunology, Institute of Microbiology, Chinese Academy of Sciences, Beijing, China; [5] The D. H. Chen School of Universal Health, Zhejiang University, Hangzhou City, Zhejiang Province, China; [6] Chinese Center for Disease Control and Prevention, Beijing, China.

Submitted: May 23, 2025
Accepted: June 19, 2025
Issued: June 27, 2025

REFERENCES

1. Gonzalez-Perez A, Landgren H, Vainio A, Kitowska W, Pihlajasaari A, Leinonen E, et al. A multi-country outbreak of *Salmonella* Mbandaka linked to pre-cooked, frozen chicken meat in ready-to-eat products, Finland, 2022 to 2023. Euro Surveill 2025;30(17):2400602. https://doi.org/10.2807/1560-7917.ES.2025.30.17.2400602.
2. U.S. Centers for Disease Control and Prevention. *Salmonella* outbreak linked to backyard poultry. 2025. https://www.cdc.gov/salmonella/outbreaks/mbandaka-05-01/index.html. [2025-5-19].
3. World Health Organization. WHO bacterial priority pathogens list, 2024: bacterial pathogens of public health importance to guide research, development and strategies to prevent and control antimicrobial resistance. Geneva: World Health Organization; 2024. https://www.who.int/publications/i/item/9789240093461.
4. Ma YY, Chen P, Mo Y, Xiao YH. WHO revised bacterial priority pathogens list to encourage global actions to combat AMR. hLife 2024;2(12):607 – 10. https://doi.org/10.1016/j.hlife.2024.10.003.
5. Xiao YH, Nishijima T. Status and challenges of global antimicrobial resistance control: a dialogue between Professors Yonghong Xiao and Takeshi Nishijima. hLife 2024;2(2):47 – 9. https://doi.org/10.1016/j.hlife.2023.11.004.
6. Wang YN, Xu XB, Jia SL, Qu MQ, Pei YH, Qiu SF, et al. A global atlas and drivers of antimicrobial resistance in *Salmonella* during 1900-2023. Nat Commun 2025;16(1):4611. https://doi.org/10.1038/s41467-025-59758-3.
7. Wang YN, Liu Y, Lyu N, et al. The temporal dynamics of antimicrobial-resistant *Salmonella enterica* and predominant serovars in China. Natl Sci Rev 2023;10(3):nwac269. https://doi.org/10.1093/nsr/nwac269.
8. Mather AE, Gilmour MW, Reid SWJ. Foodborne bacterial pathogens: genome-based approaches for enduring and emerging threats in a complex and changing world. Nat Rev Microbiol 2024;22(9):543 – 55. https://doi.org/10.1038/s41579-024-01051-z.
9. Baker S, Thomson N, Weill FX, Holt KE. Genomic insights into the emergence and spread of antimicrobial-resistant bacterial pathogens. Science 2018;360(6390):733 – 8. https://doi.org/10.1126/science.aar3777.
10. Wang YN, Xu XB, Zhu BL, Lyu N, Liu Y, Ma SF, et al. Genomic analysis of almost 8,000 *Salmonella* genomes reveals drivers and landscape of antimicrobial resistance in China. Microbiol Spectr 2023;11(6):e0208023. https://doi.org/10.1128/spectrum.02080-23.

Vital Surveillances

Epidemiological Characteristics and Spatiotemporal Cluster Analysis of Scrub Typhus — China, 2006–2023

Yao Qin[1,2,3,&]; Shijian Zhou[1,&]; Qi Wang[2,3]; Huijie Qin[1]; Junyuan Chen[1]; Sihan Li[1]; Yanping Zhang[1]; Qiulan Chen[1,#]

ABSTRACT

Introduction: Scrub typhus, also known as jungle typhus, is a vector-borne disease transmitted to humans through the bite of infected chiggers carrying *Orientia tsutsugamushi*. In recent years, it has reemerged as a significant public health concern in China, with cases being identified in an increasing number of previously unaffected regions.

Methods: Data were obtained from the China Information System for Disease Control and Prevention (CISDCP). We employed Joinpoint 5.1.0 for trend analysis and RStudio 4.4.1 for statistical analyses, including Mann-Whitney U tests (non-parametric), Cochran-Armitage tests, and binary logistic regression. SaTScan 9.1.1 and ArcGIS 10.7 were utilized to identify high-risk spatial clusters.

Results: Scrub typhus incidence in China increased dramatically from 0.095/100,000 to 2.357/100,000 between 2006 and 2023. The epidemic trend was categorized into 3 distinct phases: a rapid increase period [APC$_{2006\text{-}2013}$=37.1%, 95% confidence interval (*CI*): 31.4%, 43.0%], a slow increase period (APC$_{2014\text{-}2018}$=13.4%, 95% *CI*: 4.6%, 23.0%), and a peak-plateau period (APC$_{2019–2023}$= −0.2%, 95% *CI*: 3.2%, 3.0%), with annual cases ranging from 24,870 to 33,229. The proportion of individuals aged ≥45 years demonstrated an increasing trend (AAPC=2.0%). We identified 3 distinct seasonal patterns across China: summer, autumn, and summer-autumn patterns. This study revealed distinct spatiotemporal characteristics of scrub typhus in China, with the primary cluster concentrated in Yunnan Province and geographic expansion from southwestern, southern, and eastern regions toward central and northern China.

Conclusions: Scrub typhus incidence in China has increased substantially and has reached a peak plateau phase. The disease exhibits distinct spatiotemporal distribution patterns, necessitating targeted control measures in affected regions.

Scrub typhus, also known as jungle typhus, represents a significant public health challenge in the Asia-Pacific region. This vector-borne disease is transmitted to humans through the bite of infected chiggers carrying *Orientia tsutsugamushi* (formerly *Rickettsia tsutsugamushi*) (*1*). The first documented case of human infection with *O. tsutsugamushi* in China was identified in 1948 in Guangzhou City, Guangdong Province (*2*). By the 1980s, scrub typhus cases occurred predominantly in regions south of the Yangtze River, including Zhejiang Province in eastern China and Yunnan Province in western China (*3*). Since the 1980s, the epidemiological distribution of scrub typhus has expanded rapidly throughout China. The geographic spread has gradually extended from provincial-level administrative divisions (PLADs), south of the Yangtze River to northern PLADs, including Tianjin, Shandong, and the three northeastern PLADs (*4*). The incidence of scrub typhus has demonstrated a marked increase in recent years, rising from 0.09/100,000 in 2006 to 1.60/100,000 in 2016, yet it remains an underrecognized tropical infectious disease (*5*).

In recent years, climate change and human expansion into previously uninhabited areas have contributed to a clear upward trend in scrub typhus incidence. This study analyzed the epidemiological characteristics and spatiotemporal clustering patterns of scrub typhus in China from 2006 to 2023 to identify high-risk populations and geographic aggregation areas. These findings will provide an evidence base for local health departments to implement targeted surveillance and control strategies, and will inform the development of preventive measures for travelers to endemic regions.

METHODS

Scrub typhus data were obtained from the China Information System for Disease Control and

Prevention (CISDCP). Case definitions followed guidelines established by the Chinese Center for Disease Control and Prevention (*6*). We utilized Excel 2010 (Microsoft, Redmond, WA, USA) for data analysis and statistical visualization. Temporal trend analysis employed Joinpoint 5.1.0 to calculate the average annual percentage change (AAPC) and annual percent change (APC). Statistical analyses were conducted using RStudio (version 4.4.1, Posit, Boston, MA, USA), including Mann-Whitney U tests for non-parametric comparisons, Cochran-Armitage tests for trend analysis, and binary logistic regression modeling to examine the relationship between median interval from illness onset to case diagnosis (T_{diag}) and mortality risk. Spatial-temporal clustering analysis utilized SaTScan software (version 9.1.1, Martin Kulldorff, Boston, MA, USA) for space-time scan statistics (STSS) as developed by Kulldorff. We identified high-risk clusters of scrub typhus at the county level across four distinct time periods. Monte Carlo simulations generated *P* values using a Poisson model, while loglikelihood ratio (LLR) and relative risk (*RR*) values were calculated to test hypotheses for each scanning window. ArcGIS Desktop software (version 10.3, Esri, Redlands, California, USA) provided visualization capabilities for spatial analysis results.

RESULTS

Temporal Trends and Seasonality

Between 2006 and 2023, China reported a total of 283,102 scrub typhus cases. Of these, 272,061 cases (96.1%) received clinical diagnoses, while 11,041 cases (3.9%) were confirmed through laboratory testing. Additionally, 103 deaths were documented, yielding an average annual incidence rate of 1.12 per 100,000 individuals. The Average Annual Percentage Change demonstrates that scrub typhus incidence in China increased by an average of 19.4% annually. The Joinpoint regression model revealed 2 significant turning points in scrub typhus incidence from 2006–2023, allowing categorization into 3 distinct phases: a rapid increase period [$\text{APC}_{2006\text{–}2013}$= 37.1%, 95% confidence interval (*CI*): 31.4%, 43.0%], a slow increase period ($\text{APC}_{2014\text{–}2018}$=13.4%, 95% *CI*: 4.6%, 23.0%), and a peak-plateau period ($\text{APC}_{2019\text{–}2023}$= −0.2%, 95% *CI*: −3.2%, 3.0%) (Figure 1).

Seasonal analysis revealed that peak incidence occurred between June and November, accounting for 88.47% of total cases, while lower incidence was observed from December to May, with consistent patterns maintained across different years (Figure 2A). Analysis of the 14 PLADs with the highest case numbers, collectively representing 98.82% of all reported cases, demonstrated 3 distinct seasonal patterns throughout China: 1) Autumn pattern: This pattern exhibited a distinct single-peak configuration with maximum incidence in October-November and a brief epidemic duration, encompassing Beijing, Henan, Shandong, Anhui, and Jiangsu PLADs (Figure 2B); 2) Summer pattern: This pattern demonstrated a single peak during the summer months, with epidemics spanning June through September, including Yunnan, Sichuan, and Hunan provinces (Figure 2C); 3) Summer-autumn pattern: This pattern displayed 2 peaks occurring in June-July and September-October,

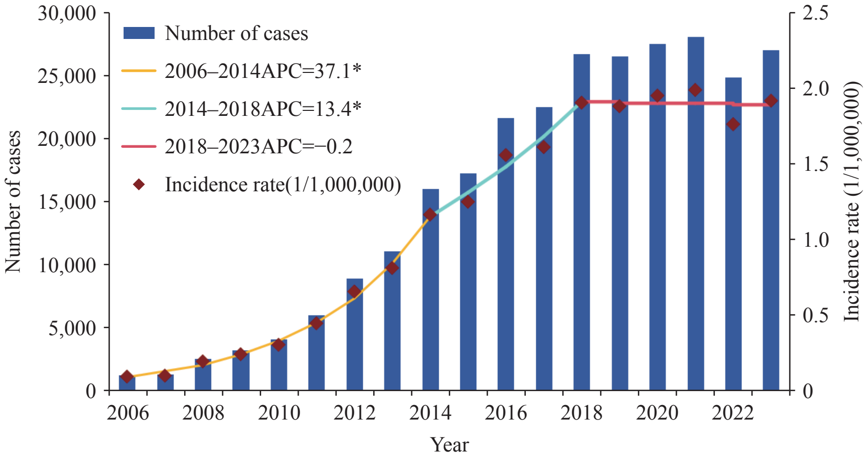

FIGURE 1. Trends in the incidence of scrub typhus, 2006–2023.
Abbreviation: APC=annual percent change.
* Indicates that the APC is significantly different from zero at the α=0.05 level (*P*<0.05).

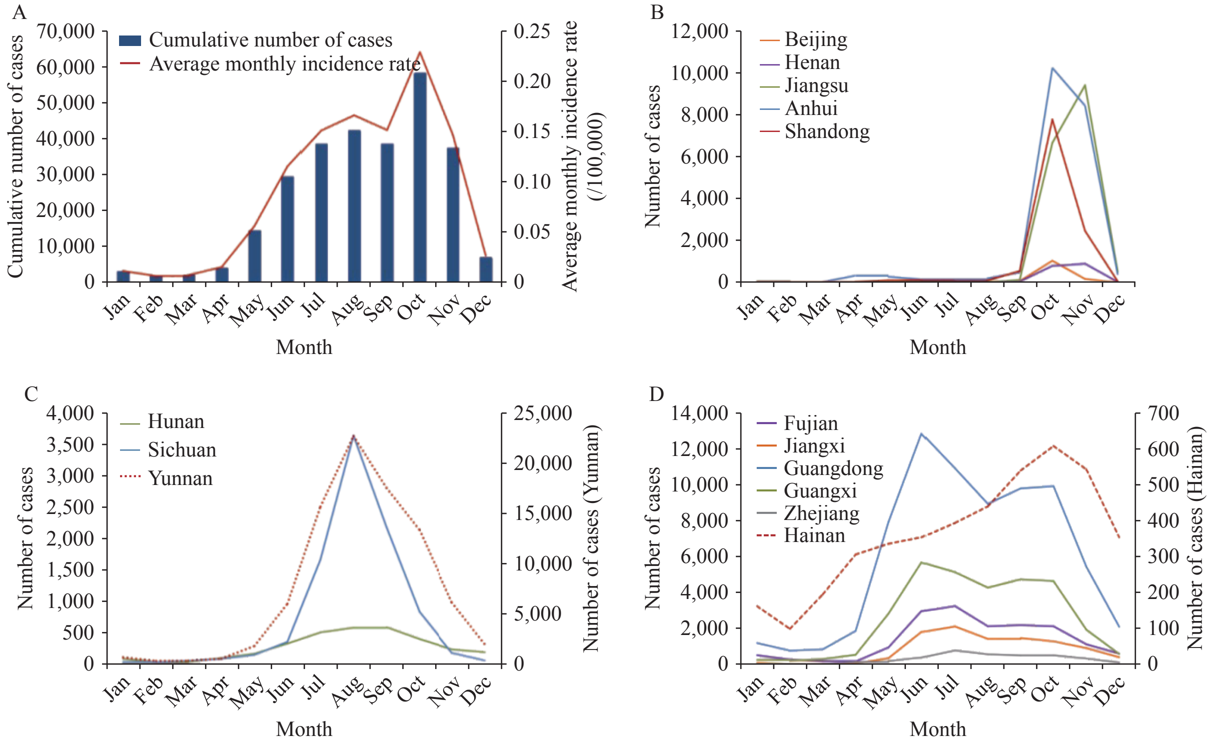

FIGURE 2. Seasonal distribution of scrub typhus cases in China, 2006–2023. (A) Seasonal distribution in China; (B) Autumn pattern; (C) Summer pattern; (D) Summer–autumn pattern.

respectively, resulting in the most extended epidemic period and including Guangdong, Guangxi, Fujian, Jiangxi, and Zhejiang PLADs (Figure 2D).

Social-Demographic Characteristics

Age distribution analysis revealed a growing proportion of individuals aged ≥45 years (AAPC=2.0%, 95% *CI*: 1.0%, 2.9%). The incidence across different age groups displayed a bimodal distribution, with peaks primarily between 55–84 years and, to a lesser extent, in the 0–9 years age bracket. The highest incidence was observed among children aged 1–5 years (Figure 3B). Regarding gender distribution, the male-to-female ratio was 0.89:1. A significant decrease in male cases was noted with advancing age (Z=−62.78, *P*<0.001), with a higher proportion of males in the 0–45 age group and more females in the ≥45 age group (Figure 3A). Occupational analysis revealed that farmers comprised the majority of cases at 76.81%, followed by children in scattered rural areas (5.30%), household members and preschool children (5.09%), and students (4.44%). There was a significant steady increase in the proportion of farmers from 2006 to 2023, rising from 60.29% to 76.69% (AAPC=1.2%, 95% *CI*: 0.7%, 1.7%).

Spatial and Temporal Distributions

The incidence of scrub typhus in China increased dramatically from 0.095/100,000 to 2.357/100,000 between 2006 and 2023. During this 18-year period, a total of 283,102 cases were reported across China. The geographic distribution was notably concentrated in 5 PLADs, which collectively accounted for 80.18% of all cases: Yunnan Province with 84,735 cases (28.87%), Guangdong Province with 69,957 cases (25.26%), Guangxi Zhuang Autonomous Region with 30,133 cases (10.88%), Anhui Province with 20,491 cases (7.40%), and Jiangsu Province with 16,765 cases (6.05%). The geographic scope of scrub typhus expanded substantially from 2006 to 2023, with affected areas growing from 217 counties/districts in 2006 to 1,086 counties/districts in 2023. To characterize the evolving geographic distribution patterns of scrub typhus in China from 2006 to 2023, we divided the study period into 4 phases: 2006–2009, 2010–2013, 2014–2018, and 2019–2023, and generated incidence maps at the county level. The analysis revealed that geographic distribution changes were minimal in 2010–2013 compared with 2006–2009. However, during 2014–2018, the geographic distribution expanded significantly from southwestern, southern, and eastern China to central

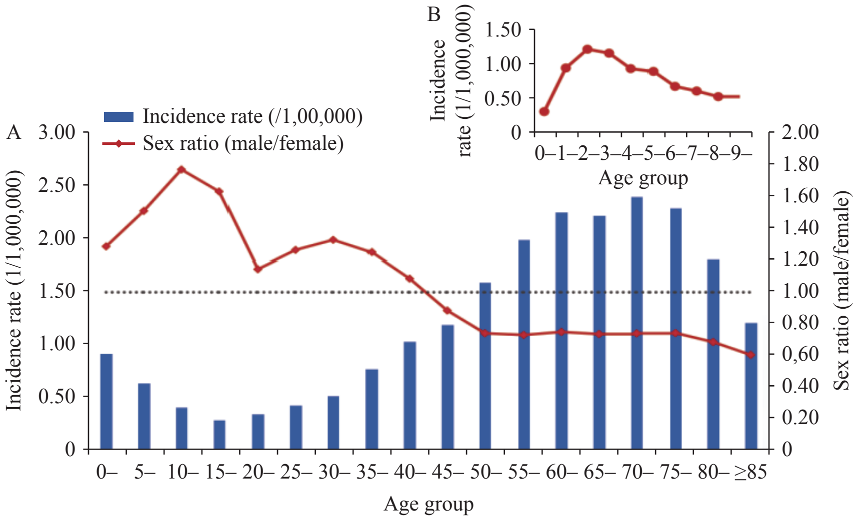

FIGURE 3. Age and sex distribution of scrub typhus. (A) Age and sex distribution of scrub typhus; (B) Incidence among children aged 0–10 years.

and northern China, with further widespread expansion occurring in 2019–2023 (Figure 4).

The spatiotemporal cluster analysis at the county level revealed distinct clustering patterns across different time periods (Supplementary Table S1, available at https://weekly.chinacdc.cn/). During 2006–2009 (Figure 4A), the primary cluster was centered in Gengma County, Yunnan Province, with a radius of 458.1 km encompassing 5 counties in Panzhihua, Sichuan Province, and 65 counties in Yunnan Province, active from June 6, 2008, to December 3, 2009. Two secondary clusters were identified: one centered in Tancheng County, Shandong Province, and another in Yangshan County, Guangdong Province, collectively affecting 134 counties across Jiangsu, Anhui, Shandong, Henan, Guangdong, Hunan, Guangxi, and Jiangxi PLADs. During 2010–2013 (Figure 4B), the primary cluster shifted to Mang City, Yunnan Province, with a 181.7 km radius covering 17 counties, active from June 6, 2012, to December 3, 2013. Two secondary clusters were centered in Yangshan County, Guangdong Province, and Weicheng County, Shandong Province, impacting a total of 228 counties across Guangdong, Guangxi, Hunan, Jiangxi, Shandong, Jiangsu, Anhui, Henan, Beijing, Hebei, Shanxi, and Tianjin. During 2014–2018 (Figure 4C), the predominant cluster was located in Menglian County, Yunnan Province, with a radius of 354.2 km, covering 44 counties from June 7, 2016, to December 3, 2018. Two secondary clusters emerged, one centered in Jinwan County, Guangdong Province, and the other in Feixian County, Shandong Province, encompassing a total of 373 counties across Guangdong, Guangxi, Hunan, Fujian, Jiangxi, Hainan, Hebei, Jiangsu, Anhui, and Shandong PLADs. During 2019–2023 (Figure 4D), the primary cluster remained in Menglian County, Yunnan Province, with a radius of 376.2 km, encompassing 47 counties from June 7, 2021, to December 3, 2023. Additionally, 3 secondary clusters emerged, centered in Pinggui County, Guangxi Zhuang Autonomous Region; Lingbi County, Anhui Province; and Taining County, Fujian Province, affecting 271 counties across Guangdong, Guangxi, Hunan, Jiangsu, Anhui, Shandong, Henan, Fujian, and Jiangxi PLADs.

Distribution of Fatal Cases and Mortality Risk Factors

During 2006–2023, 103 deaths were reported, yielding a case fatality rate of 36.4 per 100,000 cases, with fatalities documented in every year except 2009. The years with the highest mortality burden were 2016 and 2011, recording 12 and 11 deaths, respectively. The male-to-female ratio among fatal cases was 1.4:1. Age distribution was predominantly concentrated in the ≥45 years group, with 87 cases (84.5%) in this demographic. The highest case fatality rates were observed in the ≥80 years group (103.8 per 100,000), followed by the 70–74 years group (70.7 per 100,000), 75–79 years group (58.5 per 100,000), and 0–4 years group (52.6 per 100,000) (Supplementary Table S2, available at https://weekly.chinacdc.cn/).

The median interval from illness onset to case

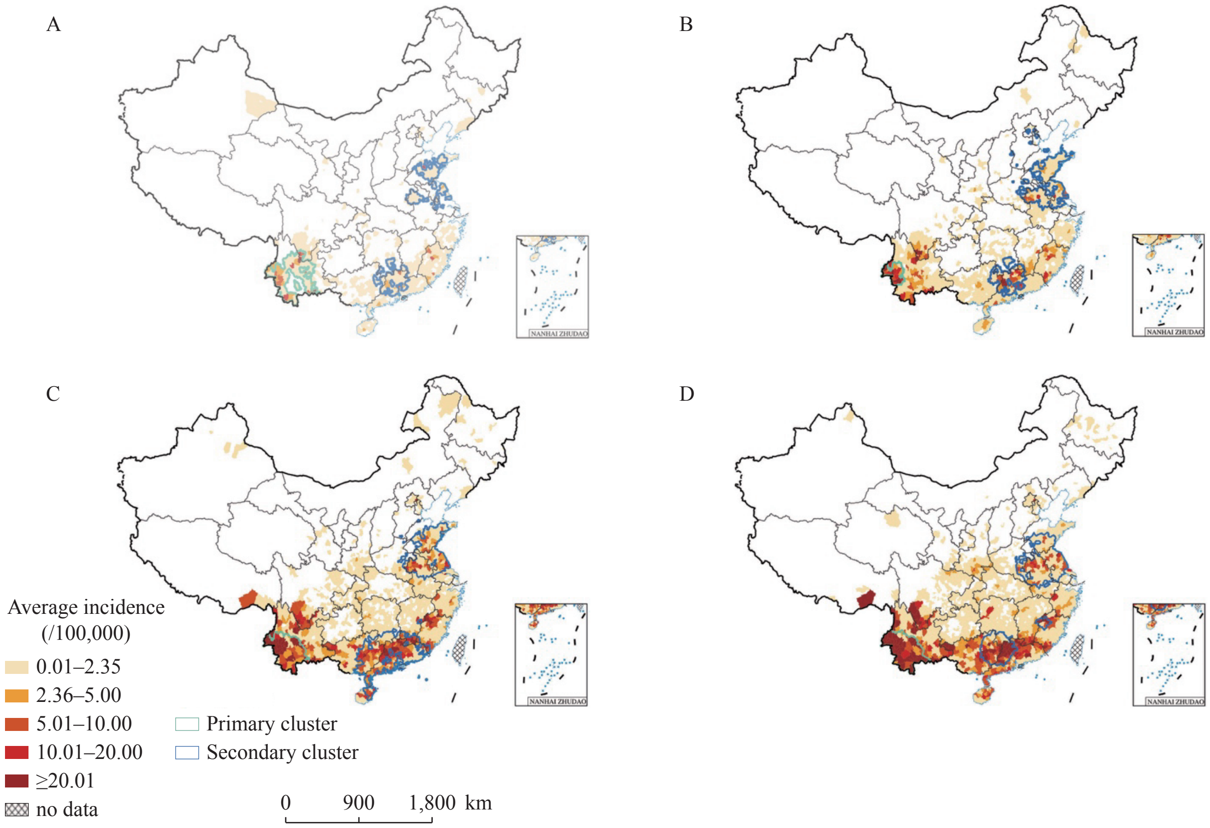

FIGURE 4. Annualized average incidence and space-time clusters of scrub typhus cases at the county level in China, 2006–2023. (A) Spatial clustering from 2006 to 2009; (B) Spatial clustering from 2010 to 2013; (C) Spatial clustering from 2014 to 2018; (D) Spatial clustering from 2019 to 2023.
Map approval number: GS 京 (2025)0900 号

diagnosis (T_{diag}) among fatal cases was 8 days [interquartile range (IQR): 4–10 days], compared to 5 days (IQR: 2–8 days) for non-fatal cases. The Mann-Whitney U-test demonstrated statistical significance ($Z=-3.586$, $P<0.001$). To investigate the effect of T_{diag} (<2 days, 2–7 days, >7 days) on mortality risk, we developed a binary logistic regression model, adjusting for covariates including gender (male, female), age group (<20, 20–39, 40–59, ≥60 years), and occupation (farmers, others, students/preschool children). Results demonstrated that cases with T_{diag} >7 days had significantly higher mortality risk than those with T_{diag} <2 days [odds ratio (*OR*)=2.0, 95% *CI*: 1.2, 3.6]. Model fit was validated using the Hosmer-Lemeshow test, which indicated good model performance ($\chi^2=12.098$, $P=0.147$). We constructed a receiver operating characteristic (ROC) curve and calculated the area under the curve (AUC) to evaluate the model's predictive capability. The AUC was 0.746 (95% *CI*: 0.6954, 0.7967), confirming the model's accuracy (Supplementary Table S3, available at https://weekly.chinacdc.cn/).

CONCLUSIONS

The incidence of scrub typhus in China increased significantly from 2006 to 2023 (AAPC=19.4%) and has now reached a peak plateau phase. We identified 3 distinct seasonal patterns across China: summer, autumn, and summer-autumn patterns. The disease predominantly affects middle-aged and elderly farmers, with gender distribution varying across age groups. The geographical distribution has progressively expanded from southwestern, southern, and eastern China to central and northern regions, with primary clusters concentrated in Yunnan Province. Cases with diagnostic delays exceeding 7 days (T_{diag}>7 days) demonstrated significantly higher mortality risk (*OR*=1.9, 95% *CI*: 1.1, 3.4).

Scrub typhus incidence has risen substantially in China and other countries, including Japan and Republic of Korea (*1*,*3*,*7*). This increase likely stems from multiple factors: advances in diagnostic techniques, human encroachment into previously uninhabited areas, and climate change (*8*–*9*). In 2009, the China CDC published the "Technical Guidelines for Prevention and Control of Tsutsugamushi (for Trial Implementation)", which standardized case reporting and enhanced diagnostic capabilities nationwide, facilitating improved case identification. Research demonstrates that urbanization has increased human exposure to vector mites, elevating infection risk (*7*). Additionally, studies suggest that rising average temperatures and increased heatwave frequency correlate with higher scrub typhus case numbers, indicating that global warming may contribute to this trend (*10*). Scrub typhus has expanded across mainland China from southwestern, southern, and eastern coastal regions to central, northern, and northeastern areas, with new endemic locations continuously identified (*4*).

The seasonal distribution of scrub typhus exhibits regional variability, consistent with several previous studies (*2*). We identified 3 distinct seasonal patterns in China: summer, autumn, and summer-autumn patterns. This variation likely relates to the population distribution and seasonal fluctuation of chigger vectors (*11*). *Leptotrombidium delicense*, *L. scutellare*, *L. sialkotense*, *L. rubellum*, *L. wenense*, and *L. insulare* have been confirmed as scrub typhus vectors in China, though many potential vectors remain unidentified (*11–13*). Vector chiggers play crucial roles in scrub typhus epidemiology and disease transmission. Therefore, strengthening nationwide chigger monitoring is essential to fully understand vector distribution in epidemic regions. The age distribution primarily affects the 45–70-year age group, with occupational distribution mainly among farmers, aligning with numerous domestic and international studies (*4*,*10*,*14*). However, unlike other research (*8*), we observed higher male proportions in the 0–44 age group, while females predominated in the ≥45 age group. This pattern may reflect middle-aged male migration to urban areas for employment, leaving women and elderly individuals in rural areas where increased agricultural activities heighten scrub typhus exposure. The slight peak in scrub typhus incidence among children aged 0–9 years can be attributed to several factors: guardians may bring children to fields during labor, and children's limited self-protection awareness increases disease exposure risk. Additionally, because children receive more intensive care and attention, illness detection occurs more readily. Misdiagnosis or delayed diagnosis can have severe consequences in children due to their lower immunity, necessitating heightened clinical attention.

Despite the availability of specific antimicrobial treatments for scrub typhus, the absence of distinctive clinical symptoms complicates its differentiation from other febrile illnesses, including dengue fever, severe fever with thrombocytopenia syndrome, and leptospirosis. Misdiagnosis or delayed diagnosis may result in severe complications and increased mortality (*8*). Our study demonstrated that patients with T_{diag} >7 days had a 1.9-fold increased mortality risk compared to those diagnosed within 2 days, consistent with findings from other investigations (*15*). Therefore, diagnostic delays significantly elevate the risk of death. As scrub typhus continues to spread to emerging regions, enhanced training programs focusing on scrub typhus diagnosis should be developed for healthcare providers in these areas.

This research has several limitations. First, scrub typhus was incorporated into the infectious disease surveillance system in 2006, but standardized reporting criteria were not established until the release of 'Technical Guidelines for Prevention and Control of Tsutsugamushi (for Trial Implementation)' in 2009, which may have compromised reporting quality during the initial period. Second, the data originated from a passive surveillance system, potentially resulting in underreporting and misreporting that could affect data accuracy. Third, this study lacked vector and host data, which are considered important variables influencing disease transmission dynamics.

In conclusion, scrub typhus in China has reached a peak plateau with expanding epidemic regions. Therefore, comprehensive control measures must be implemented. These measures should include enhanced physician training in diagnosis and treatment, particularly in newly emerging areas, to ensure timely case detection. Additionally, increased public awareness and education campaigns in endemic areas can guide at-risk populations in adopting appropriate protective measures.

Conflicts of interest: No conflicts of interest.

Funding: Supported by the Public Health Emergency Response Mechanism Operation Program of the Chinese Center for Disease Control and Prevention (102393220020010000017), Chinese National Science and Technology Major Project (No.2018ZX10101002-003-002).

doi: 10.46234/ccdcw2025.146

Corresponding author: Qiulan Chen, chenql@chinacdc.cn.

---

[1] National Key Laboratory of Intelligent Tracking and Forecasting for Infectious Diseases, Chinese Center for Disease Control and

Prevention, Beijing, China; [2] Chinese Field Epidemiology Training Program, Chinese Center for Disease Control and Prevention, Beijing, China; [3] Sichuan Center for Disease Control and Prevention, Chengdu City, Sichuan Province, China.
[&] Joint first authors.

Submitted: February 05, 2025
Accepted: June 20, 2025
Issued: June 27, 2025

REFERENCES

1. Xu G, Walker DH, Jupiter D, Melby PC, Arcari CM. A review of the global epidemiology of scrub typhus. PLoS Negl Trop Dis 2017;11(11):e0006062. https://doi.org/10.1371/journal.pntd.0006062.
2. Li ZJ, Xin HL, Sun JL, Lai SJ, Zeng LJ, Zheng CJ, et al. Epidemiologic changes of scrub typhus in China, 1952-2016. Emerg Infect Dis 2020;26(6):1091 – 101. https://doi.org/10.3201/eid2606.191168.
3. Wu YC, Qian Q, Soares Magalhaes RJ, Han ZH, Hu WB, Haque U, et al. Spatiotemporal dynamics of scrub typhus transmission in mainland China, 2006-2014. PLoS Negl Trop Dis 2016;10(8):e0004875. https://doi.org/10.1371/journal.pntd.0004875.
4. Zhang M, Wang XJ, Zhao ZT. Current epidemic status and issues on prevention and control of scrub typhus. Chin J Epidemiol 2011;32(4):419 – 23. https://doi.org/10.3760/cma.j.issn.0254-6450.2011.04.021.
5. Qian L, Wang Y, Wei XY, Liu P, Magalhaes RJS, Qian Q, et al. Epidemiological characteristics and spatiotemporal patterns of scrub typhus in Fujian province during 2012-2020. PLoS Negl Trop Dis 2022;16(9):e0010278. https://doi.org/10.1371/journal.pntd.0010278.
6. Chinese Centre for Disease Control and Prevention. Technical guidelines for the prevention and control of scrub typhus (Trial), 2009. https://www.doc88.com/p-943564041043.html.[2024-05-23]. (In Chinese).
7. Chang T, Min KD, Cho SI, Kim Y. Associations of meteorological factors and dynamics of scrub typhus incidence in South Korea: a nationwide time-series study. Environ Res 2024;245:117994. https://doi.org/10.1016/j.envres.2023.117994.
8. Kinoshita H, Arima Y, Shigematsu M, Sunagawa T, Saijo M, Oishi K, et al. Descriptive epidemiology of rickettsial infections in Japan: scrub typhus and Japanese spotted fever, 2007-2016. Int J Infect Dis 2021;105:560 – 6. https://doi.org/10.1016/j.ijid.2021.02.069.
9. Ding FY, Wang Q, Hao MM, Maude RJ, John Day NP, Lai SJ, et al. Climate drives the spatiotemporal dynamics of scrub typhus in China. Glob Chang Biol 2022;28(22):6618 – 28. https://doi.org/10.1111/gcb.16395.
10. Bonell A, Lubell Y, Newton PN, Crump JA, Paris DH. Estimating the burden of scrub typhus: a systematic review. PLoS Negl Trop Dis 2017;11(9):e0005838. https://doi.org/10.1371/journal.pntd.0005838.
11. Chen AX, Tian C, Yang X, Cao G, Lyu XF. Research progress on the distribution of scrub typhus vector chigger mites in China. Chin J Hyg Insect Equip 2022;28(6):556 – 61. https://doi.org/10.19821/j.1671-2781.2022.06.021.
12. Wu GH, Jiang ZK, Wang L, Ding LY, Mao CQ, Ma BY. Accordance and identification of vector chigger mites of tsutsugamushi disease in China. Chin J Hyg Insect Equip 2013;19(4):286 – 92. https://doi.org/10.19821/j.1671-2781.2013.04.004.
13. Stekolnikov AA. *Leptotrombidium* (Acari: Trombiculidae) of the world. Zootaxa 2013;3728:1 – 173. https://doi.org/10.11646/zootaxa.3728.1.1.
14. Xin HL, Yu JX, Hu MG, Jiang FC, Li XJ, Wang LP, et al. Evaluation of scrub typhus diagnosis in China: analysis of nationwide surveillance data from 2006 to 2016. Infect Dis Poverty 2019;8(1):59. https://doi.org/10.1186/s40249-019-0566-0.
15. Jin HS, Chu C, Han DY. Spatial distribution analysis of scrub typhus in Korea. Osong Public Health Res Perspect 2013;4(1):4 – 15. https://doi.org/10.1016/j.phrp.2012.12.007.

SUPPLEMENTARY MATERIAL

SUPPLEMENTARY TABLE S1. Space-time clusters of scrub typhus in China, 2006–2023.

Scan time (year)	Cluster type	Cluster time (yyyy/mm/dd)	Cluster counties (*n*)	Centroid (latitude, longitude)/ radius (km)	LLR	*RR*	*P*
2006–2009	1	2008/6/6–2009/12/3	68	(23.639066 N, 99.425054 E) / 458.1 km	1,924.1	9.3	<0.001
	2	2008/10/10–2008/11/6	76	(34.626866 N, 118.317619 E) / 354.0 km	826.1	15.7	<0.001
	3	2009/5/22–2009/10/8	58	(24.506085 N, 112.670218 E) / 214.2 km	486.5	6.4	<0.001
2010–2013	1	2012/6/6–2013/12/3	17	(24.326062 N, 98.420482 E) / 181.7 km	5,579.7	25.0	<0.001
	2	2012/5/9–2013/11/5	65	(24.506085 N, 112.670218 E) / 218.7 km	3,634.2	5.8	<0.001
	3	2013/10/9–2013/11/19	163	(36.696422 N, 119.021632 E) / 546.6 km	2,158.1	9.0	<0.001
2014–2018	1	2016/6/7–2018/12/3	44	(22.290364 N, 99.468614 E) / 354.2 km	26,969.5	18.1	<0.001
	2	2016/5/10–2018/11/5	203	(22.042525 N, 113.257495 E) / 475.7 km	8,692.4	3.0	<0.001
	3	2016/10/11–2016/11/21	170	(35.244147 N, 117.937790 E) / 365.8 km	6,569.5	11.1	<0.001
	4	2015/6/9–2017/12/4	1	(27.112472 N, 116.488972 E) / 0 km	2,098.5	38.4	<0.001
2019–2023	1	2021/6/7–2023/12/3	47	(22.290364 N, 99.468614 E) / 376.2 km	64,937.2	30.5	<0.001
	2	2019/5/13–2021/11/7	69	(24.298720 N, 111.432178 E) / 202.2 km	12,006.6	5.9	<0.001
	3	2019/10/14–2019/11/10	194	(33.686076 N, 117.531189 E) / 314.1 km	6,645.7	12.1	<0.001
	4	2019/5/13–2021/11/7	8	(26.861849 N, 117.113375 E) / 74.4 km	1,111.4	8.1	<0.001

Note: The cluster with the maximum LLR is the primary cluster, and the other clusters are secondary.
Abbreviation: LLR=Log likelihood ratio; *RR*=relative risk.

SUPPLEMENTARY TABLE S2. Age distribution of fatal cases of scrub typhus in China, 2006–2023.

Age group (year)	Number of cases	Number of deaths	Case fatality rates (/100,000)
0–	13,299	7	52.6
5–	8,960	0	0
10–	5,622	0	0
15–	3,687	1	27.1
20–	4,915	2	40.7
25–	8,004	0	0
30–	11,201	1	8.9
35–	13,884	1	7.2
40–	18,364	4	21.8
45–	26,434	8	30.3
50–	34,290	9	26.2
55–	34,107	15	44.0
60–	31,607	13	41.1
65–	28,282	12	42.4
70–	19,802	14	70.7
75–	11,973	7	58.5
80–	8,671	9	103.8
Total	283,102	103	36.4

SUPPLEMENTARY TABLE S3. Mortality risk factors of scrub typhus in China, 2006–2023.

Grouping of variables		Multifactorial analysis		
		Wald χ^2	***OR* (95% *CI*)**	***P***
Gender	Female			
	Male	4.135	1.5 (1.0–2.2)	0.042
Age group (years)	<20	17.391		
	20–39	1.870	0.2 (0.1–1.9)	0.171
	40–59	0.035	0.8 (0.1–5.8)	0.851
	≥60	0.150	1.5 (0.2–10.2)	0.698
Occupation	Farmer	62.760		
	Students/preschool children	61.690	5.1 (3.4–7.6)	<0.001
	others	0	1.0 (0.1–7.7)	0.983
Tdiag (days)	<2	10.469		
	2–7	0.031	1.1 (0.6–1.9)	0.860
	>7	5.618	2.0 (1.2–3.6)	0.018

Preplanned Studies

Niche Analysis of Spatial Distribution and Host Selection of Global *Echinococcus* Species — Worldwide, up to June 30, 2024

Xu Wang[1,2]; Qingqiu Zuo[1]; Chuizhao Xue[1]; Baixue Liu[1]; Yan Kui[1]; Xueying Deng[3]; Yang Yang[4,5];
Mengqing Li[1]; Shuai Han[1,6,#]; Zhenghuan Wang[7,#]; Yujuan Shen[1]; Jianping Cao[1,4,5]

Summary

What is already known about this topic?

Echinococcosis is a serious public health concern caused by *Echinococcus* larvae. To date, 10 *Echinococcus* species have been identified globally, each with potential variations in geographic distribution and host selection.

What is added by this report?

This study presented the provincial-level distribution of all *Echinococcus* species globally and constructed a host frequency matrix for them. By quantifying both spatial and host niches, it provides comprehensive data for understanding the ecological adaptability of *Echinococcus* species and the transmission patterns of echinococcosis.

What are the implications for public health practice?

This study's results highlight the interspecific heterogeneity and associations among different *Echinococcus* species, suggesting the need for targeted approaches in epidemiological investigations, source tracing, and risk surveillance to effectively control echinococcosis.

ABSTRACT

Objective: Echinococcosis is a fatal parasitic disease caused by infection with the larval stages of *Echinococcus* spp.. This study explored the spatial distribution characteristics and the host selection patterns of global *Echinococcus* species based on niche analysis, to provide scientific insights for the prevention and control of echinococcosis.

Methods: Relevant literature was retrieved from Web of Science, PubMed, ScienceDirect, and CNKI (China National Knowledge Infrastructure) databases. Data on the host information and geographic locations for all *Echinococcus* species worldwide were extracted. The spatial distribution characteristics of *Echinococcus* were summarized, and the host frequency heatmaps were generated using the SRplot platform. Niche indices were calculated and visualized using R language packages and the Hiplot Pro platform.

Results: The ten existing *Echinococcus* species were documented across 1,770 provincial-level administrative divisions in 113 countries, involving 188 species of host animals. Significant heterogeneity with varying degrees of overlap and differentiation was observed in spatial and host niches among *Echinococcus* species. The overall spatial distribution among *Echinococcus* species showed a significantly negative correlation (VR=0.85, W=1,502.79<χ^2 0.951770), while host selection patterns revealed no significant correlation (VR=0.90, χ^2 0.95187<W=167.70<χ^2 0.05187). *Echinococcus granulosus* and *Echinococcus multilocularis* exhibited the broadest spatial niche (B_{Eg}=7.34) and host niche (B_{Em}=3.07), respectively.

Conclusion: The spatial distribution and host selection among *Echinococcus* species exhibit complex heterogeneity and correlations, requiring the development of targeted strategies for the prevention, control, and surveillance of echinococcosis.

Echinococcosis is a deadly infectious disease caused by *Echinococcus* larvae infection (*1*). Understanding the ecological niche of *Echinococcus* is crucial for exploring echinococcosis epidemiology. This study retrieved infection events and investigations of all 10 *Echinococcus* species from databases and found that *Echinococcus* spp. are currently distributed in at least 1,770 provincial regions across 113 countries, with 188 mammalian host species globally. Significant heterogeneity exists in the geographical distribution and host selection among different *Echinococcus* species. The niche overlap and separation of *Echinococcus* species contribute to the complexity, diversification, and endemicity of echinococcosis. These findings suggest that current surveillance approaches should be reconsidered and that differences among *Echinococcus* species must be fully accounted for in echinococcosis control. Specific host surveillance, targeted control strategies, and precise epidemiological investigations should be tailored to different types of endemic areas.

Echinococcosis causes approximately 19,300 deaths and 871,000 disability-adjusted life years, and costs more than 3 billion United States Dollars (USD) worldwide per year (*2*). Recent studies have recognized 10 valid natural species of *Echinococcus* worldwide: *Echinococcus granulosus* (*Eg*), *E. equinus* (*Ee*), *E. ortleppi* (*Eor*), *E. intermedius* (*Ei*), *E. canadensis* (*Ec*), *E. felidis* (*Ef*), *E. multilocularis* (*Em*), *E. shiquicus* (*Es*), *E. vogeli* (*Ev*), and *E. oligarthra* (*Eol*) (*1*). Host suitability and geographical distribution vary significantly among these *Echinococcus* species; however, detailed information remains limited due to a lack of systematic molecular data (*3*).

In this study, researchers conducted a comprehensive literature search from the Web of Science (https://webofscience.clarivate.cn), PubMed (https://pubmed.ncbi.nlm.nih.gov), ScienceDirect (https://www.sciencedirect.com/), and the China National Knowledge Infrastructure (https://www.cnki.net/) databases using the search terms "*Echinococcus*," "echinococcosis," "hydatid disease," and "hydatidosis." The final search was completed on June 30, 2024. This study's authors performed full-text reviews and included articles with detailed investigation locations and clear identification of *Echinococcus* species/genotypes or echinococcosis types. Data on *Echinococcus* species, host species, and discovery locations (provincial-level administrative divisions, PLADs) were then extracted for subsequent analyses. The heat map of host occurrence frequencies was generated using the SRplot platform (https://www.bioinformatics.com.cn). Four ecological indices were calculated and visualized using the spaa package in R version 4.1.3 (R Core Team, Vienna, Austria) and Hiplot Pro platform (https://hiplot.com.cn): Shannon's niche width (breadth) index (B_i), Levin's niche overlap index ($O_{i\text{-}k}$), the overall interspecific association quantified by the variance ratio (VR) and tested for significance using the statistic W, and interspecific association coefficient (AC).

According to globally available data from 285 formal publications, 10 *Echinococcus* species have been reported in 1,770 provincial administrations across 113 countries (34 in Asia, 41 in Europe, 21 in Africa, 5 in North America, 11 in South America, and 1 in Oceania) (Supplementary Material, available at https://weekly.chinacdc.cn/). *Echinococcus* spp. have been observed or detected in 188 host species from 25 families, comprising 157 species (94 rodents, 34 ungulates, 18 marsupials, 7 primates, and 4 insectivores) serving as intermediate hosts (IHs) and 30 species (17 canids, 12 felids, and 1 quoll) acting as definitive hosts (DHs). Humans are considered accidental hosts and play a dead-end role in the life cycle of *Echinococcus* spp. (Figure 1).

Among the 10 *Echinococcus* species, *Eg* was the most extensively documented across 93 countries (Asia, Europe, Africa, Oceania and the Americas), with dogs serving as the primary DHs (95.52% of all DH occurrences) and Bovidae animals as the predominant IHs (89.81% of all IH occurrences). *Em* was identified in 58 countries (Asia, Europe and North America), with foxes (47.26%) and dogs (35.98%) as the main DHs, and rodents as the principal IHs (93.83%). *Ei* was reported in 52 countries (Asia, Europe, Africa and South America), with dogs (61.29%) as the primary DHs, and camels (26.12%) and pigs (22.39%) as the main IHs. *Eor* was found in 35 countries (Asia, Europe, Africa and Latin America), with dogs (75.00%) as the predominant DHs, and cattle (57.89%) and pigs (11.58%) as the main IHs. *Ec* was identified in 10 countries in northern Asia, Europe and North America, with wolves (78.95%) and coyotes (21.05%) as DHs and Cervidae animals (96.43%) as IHs. *Ee* was recorded in 17 countries (western and southern Europe, western and central Asia, eastern and southern Africa), with dogs (60.00%) as the main DHs and Equidae animals (75.76%) as the principal IHs. *Ev* was documented in 10 countries in northern South America, with *Speothos venaticus* (85.71%) and *Cuniculus paca* (63.64%) being the main DH and IH, respectively. *Eol* was recorded in 8 countries in Latin America, with agouties (54.55%) as the main IHs and *Puma concolor* (33.33%) and other American Feline animals as the DHs. *Ef* was found in 5 countries (Kenya, Namibia, Uganda, Zambia and South Africa) in Sub-Saharan Africa, with lions (73.33%) being the preferred DHs, and warthogs and hippopotamuses as the few documented IHs. *Es* is currently considered endemic to the Tibetan Plateau in China, with *Ochotona curzoniae* (66.67%) and *Vulpes ferrilata* (42.86%) being the main IH and DH, respectively. Additionally, the most frequent cause of human echinococcosis was *Eg* (69.45%), followed by *Em* (10.24%), *Ei* (9.04%), *Eor* (4.78%), *Ev* (3.75%), *Eol* (1.19%), *Ec* (0.85%), and *Ee* (0.68%), whereas *Es* and

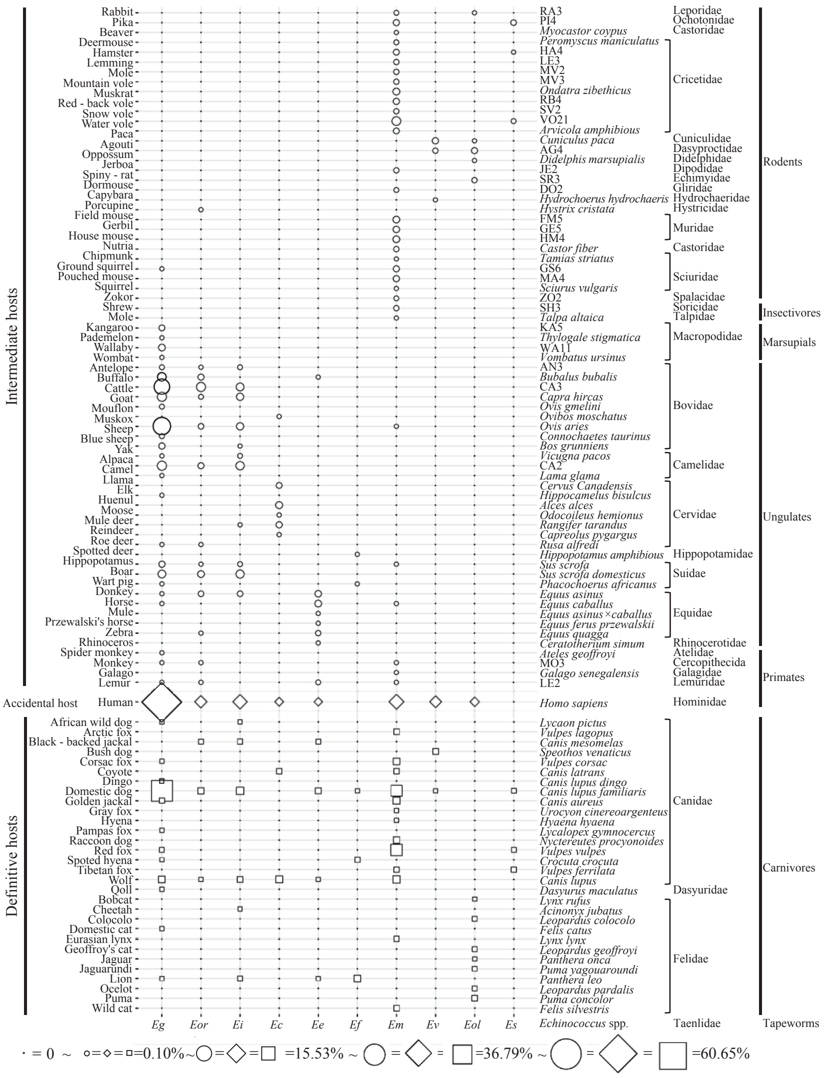

FIGURE 1. The heatmap for host occurrence frequencies of 10 *Echinococcus* species.

Note: A separate information pool was created for each *Echinococcus* species, encompassing all reported host species within each provincial district (with each host species recorded only once per PLAD). The statistics for intermediate hosts, definitive hosts, and humans within each information pool were treated independently. Occurrence frequency = (the number of occurrences of the species/the total number of occurrences of all species recorded in the information pool) × 100%. RA3: *L. europaeus*, *L. oiostolus*, *Sylvilagus floridanus*; PI4: *Ochotona dauurica*, *O. pallasii*, *O. rufescens*, *O. curzoniae*; HA4: *Cricetulus barabensis*, *C. kamensis*, *C. migratorius*, *C. longicaudatus*; LE3: *Lemmus lemmus*, *L. sibiricus*, *Dicrostonyx torquatus*; MV2: *Ellobius talpinus*, *E. tancrei*; MV3: *Alticola argentatus*, *A. olchonensis*, *A. strelzovi*; RB4: *Myodes rutilus*, *M. rex*, *M. rufocanus*, *Clethrionomys gapperi*; SV2: *Chionomys nivalis*, *C. roberti*; VO21: *Alexandromys limnophilus*, *A. middendorffii*, *A. oeconomus*, *Blanfordimys juldaschi*, *Lagurus lagurus*, *Lasiopodomys brandtii*, *L. gregalis*, *Microtus agrestis*, *M. arvalis*, *M. guentheri*, *M. ilaeus*, *M. irani*, *M. mystacinus*, *M. pennsylvanicus*, *M. socialis*, *M. subterraneus*, *M. transcaspicus*, *Myodes glareolus*, *Neodon irene*, *N. leucurus*, *N. fuscus*; AG4: *Dasyprocta leporina*, *D. azarae*, *D. punctata*, *D. fuliginosa*; JE2: *Pygeretmus pumilio*, *Scarturus elater*; SR3: *Proechimys guyannensis*, *P. trinitatus*, *P. semispinosus*; DO2: *Dryomys nitedula*, *Eliomys quercinus*; FM5: *Apodemus agrarius*, *A. argenteus*, *A. sylvaticus*, *A. uralensis*, *A. witherbyi*; GE5: *Meriones libycus*, *M. meridianus*, *M. persicus*, *M. unguiculatus*, *Rhombomys opimus*; HM4: *Mus macedonicus*, *M. musculus*, *Nesokia indica*, *Rattus norvegicus*; GS6: *Spermophilus alashanicus*, *S. erythrogenys*, *S. pygmaeus*, S. relictus, *Urocitellus undulates*. MA4: *Marmota baibacina*, *M. bobak*, *M. caudata*, *M. marmota*; ZO2: *Eospalax fontanierii*, *Myospalax myospalax*. SH3: *Sorex unguiculatus*, *S. jacksoni*, *Crocidura suaveolens*; KA5: *Macropus giganteus*, *M. rufogriseus*, *M. fuliginosus*, *M. dorsalis*, *Dendrolagus lumholtzi*; WA11: *Macropus parryi*, *Notamacropus dorsalis*, *N. parryi*, *N. rufogriseus*, *Onychogalea fraenata*, *Osphranter robustus*, *Petrogale godmani*, *P. mareeba*, *P. penicillata*, *P. persephone*, *Wallabia bicolor*; AN3: *Addax nasomaculatus*, *Gazella gazelle*, *Oryx gazelle*; CA3: *Bos taurus*, *B. indicus*, *B. frontalis*; CA2: *Camelus dromedaries*, *C. bactrianus*; MO3: *Cercopithecus ascanius*, *Pygathrix nemaeus*, *Macaca sylvanus*; LE2: *Lemur catta*, *Varecia rubra*.

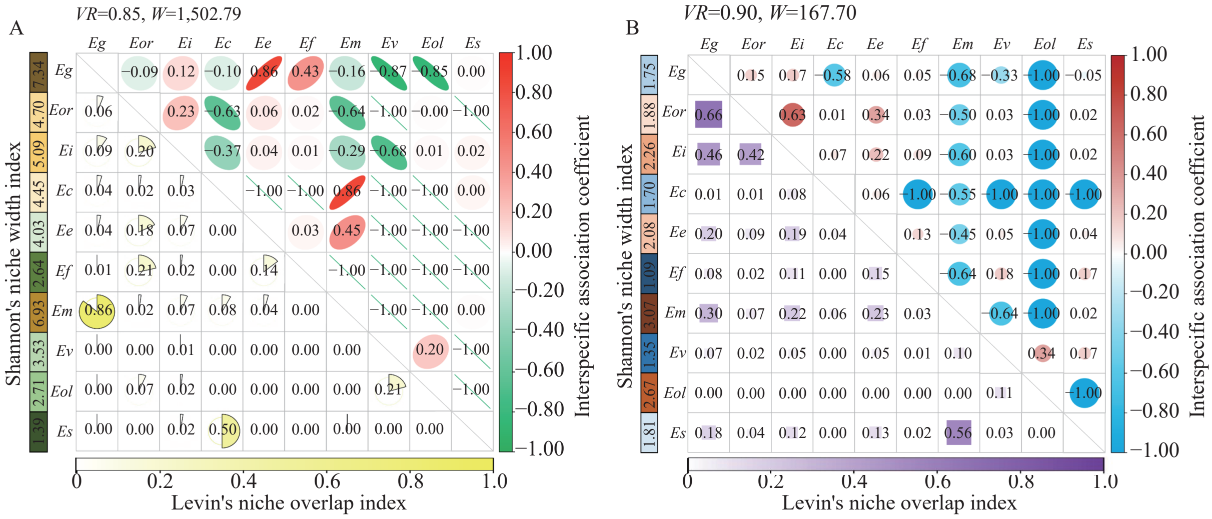

FIGURE 2. The spatial and host niche indexes of 10 *Echinococcus* species. (A) the spatial niche indexes; (B) the host niche indexes.

Note: Shannon's niche width (breadth) index (B_i)=$-\sum_{j=1}^{N}(P_{ij}\times \mathrm{Ln}P_{ij})$; Levin's niche overlap index (O_{ik})=$\frac{\sum_{j=1}^{N}(P_{ij}\times P_{kj})}{\sum_{j=1}^{N}(P_{ij})^2}$; variance ratio ($VR$)=$\frac{1/N\sum_{j=1}^{N}(T_j-t)^2}{\sum_{i=1}^{s}[(n_i/N)\times(1-n_i/N)]}$; Statistic W=VR*N; interspecific association coefficient (AC)=$\frac{a\times d-b\times c}{(a+b)\times(b+d)}$ (if $a*d \geq b*c$) or $\frac{a\times d-b\times c}{(a+b)\times(a+c)}$ (if $a*d < b*c$ and $a \leq d$) or $\frac{a\times d-b\times c}{(b+d)\times(d+c)}$ (if $a*d < b*c$ and $a > d$); i and k represents the *Echinococcus* species (i) and (k), respectively; j represents the space (PLAD) (j) or host species (j); N represents the number of spaces (PLADs) or host species; P_{ij} and P_{kj} represents abundance of species (i) and (k) for (j), respectively; S represents the number of *Echinococcus* species; n_i represents the number of spaces (PLADs) or host species that (i) appears; T_j represents the number of *Echinococcus* species for (j); t represents the mean number of *Echinococcus* species for all spaces (PLADs) or host species; a represents the number of spaces (PLADs) or host species occupied both by (i) and (k); b represents the number of spaces (PLADs) or host species occupied only by (i); c represents the number of spaces (PLADs) or host species only have (k); d represents the number of spaces (PLADs) or host species without (i) or (k); B_i represents the niche width of species (i), with a higher value indicating a wider niche; O_{ik} denotes the index of niche overlap between *Echinococcus* species of (i) and (k), with a higher value indicating more niche overlap; VR refers variance ratio of the number to the relative frequency of *Echinococcus* species, with a value >1 indicating a positive overall interspecific association and a value <1 indicating negative association; W is used in comparison with chi square (χ^2) threshold with N, with a value $>\chi^2$ (P=0.05) or χ^2 (P=0.95) indicating a significant overall interspecific association and a value $<\chi^2$ (P=0.05) and $>\chi^2$ (P=0.95) indicating an insignificant association; AC represents interspecific association between each pair of species, with a value >1 indicating a positive association and a value <1 indicating negative association.
Abbreviation: PLAD=provincial-level administrative division.

Ef have not yet been recorded in humans (Figure 1 and Supplementary Material).

In terms of the spatial niche, *Eg* exhibited the largest niche width (B_{Eg}=7.34), with niche overlap with nearly all other species (mean $O_{Eg\text{-}others}$=0.12±0.28), particularly with *Em* ($O_{Eg\text{-}Em}$=0.86). Conversely, the niche overlaps between *Ev* and other species were the lowest ($O_{mean\text{-}Ev}$=0.02±0.06), and *Es* showed the smallest niche width (B_{Es}=1.39). For the host (excluding humans) niche, *Em* had the largest niche width (B_{Em}=3.07), whereas *Ef* had the smallest niche width (B_{Ef}=0.03). The group comprising *Eg*, *Eor*, and *Ei* (mean $O_{Eg\text{-}Eor\text{-}Ei}$=0.64±0.04) and that comprising *Em* and *Es* ($O_{Em\text{-}Es}$=0.56) exhibited higher niche overlaps. The overall interspecific association of spatial distribution among *Echinococcus* species (VR=0.85, W=1,502.79) showed significant negative associations, with 14 (AC>0) and 31 (AC<0) pairs of positive and negative correlations, respectively, in all interspecific correlations. The overall interspecific association of host selection (VR=0.90, W=167.70) showed no significant associations, with 16 positive and 29 negative pairs (Figure 2).

To date, human echinococcosis caused by *Eg*, *Em*, *Ei*, *Ec*, and *Eor* has been identified in China. These findings will facilitate the development of targeted, differentiated, and localized control and surveillance strategies to address the complex epidemiology of echinococcosis.

DISCUSSION

Notably, *Eg* is the most common cause of cystic echinococcosis (CE) globally, followed by *Ei*, which also has a widespread global distribution. Additionally, *Eor*, *Ec*, and *Ee* can cause endemic CE. *Eor* is primarily concentrated in the tropical and subtropical regions, *Ec* is mainly distributed in the frigid and sub-frigid zones, and *Ee* is more common in the temperate and tropical grasslands. Furthermore, *Em* causes alveolar echinococcosis (AE) in the Northern Hemisphere, while *Ev* and *Eol* cause polycystic and unicystic echinococcosis, respectively, in the neotropical regions. *Ef* and *Es* are confined to sub-Saharan Africa and the Tibetan Plateau in China, respectively (*4*). The significant negative association in spatial distribution suggests the existence of interspecific competition or differentiation for habitat utilization among different *Echinococcus* species.

The main intermediate hosts of *Eg*, *Ei*, and *Eor* are Bovidae, Camelidae, and Suidae; however, *Eg* is also susceptible to marsupials, and both *Eg* and *Eor* can infect primates. *Ec* and *Ee* prefer Cervicidae and Equidae as intermediate hosts, respectively. Interestingly, the definitive hosts of *Ec* have only been recorded in wild canids (wolves and coyotes), whereas *Ee* has been found in both domestic and wild canids (dogs, wolves, and jackals). The intermediate hosts of *Em*, *Es*, *Ev*, and *Eol* are mainly native rodents from Eurasia, the Tibetan Plateau, South America, and Latin America, respectively. *Em*, *Es*, *Ec*, *Ef*, and *Eol* are the five species that can complete their life cycles through predation by wild animals, with *Ec*, *Ef*, and *Eol* even capable of parasitizing exclusively in wildlife. Additionally, *Ef* and *Eol* rely on feline animals as their primary definitive hosts for transmission (*5*). Dog infections have not been recorded for *Ec* and *Eol*. This study's results demonstrate a relatively independent host selection pattern with loose interspecific association among the different *Echinococcus* species.

Notably, *Eg* had the widest spatial niche, indicating its exceptional adaptability to diverse habitats. It is found on almost all continents inhabited by humans and represents the dominant pathogen causing human echinococcosis, primarily due to its main hosts (dogs and livestock) which can migrate globally with human activities. However, a disadvantage of its host niche is that the transmission chain of *Eg* is relatively fragile. Interventions targeting dog infections or improving livestock slaughter management can effectively contain CE epidemics caused by *Eg*. In contrast, *Em* demonstrates a significant advantage in host niche breadth, revealing a highly complex lifecycle involving numerous host species, particularly wildlife. Consequently, AE caused by *Em* exhibits diverse and unpredictable transmission pathways, posing substantial challenges to disease control efforts (*6*).

However, limitations in development level, technical capabilities, and research priorities have resulted in many countries and regions lacking comprehensive surveillance systems for echinococcosis and molecular data on *Echinococcus* species, making it difficult to determine the actual prevalence of this zoonotic disease in detail (*7*). In particular, this study cannot definitively establish the presence or absence of *Echinococcus* species in areas without confirmed research. Therefore, in this study, its authors focused on distribution at intercontinental geographical scales and climatic zone levels, using maximum boundaries to describe the spatial characteristics of *Echinococcus*.

This study highlights the need for adaptive adjustments to surveillance and control programs based on local echinococcosis epidemiology. For example, host surveillance for CE caused by *Eor* in southwest China (Yunnan, Guangxi, and Guizhou) should equally consider pigs in addition to cattle (*8*). Regarding the emergence of *Ec*-induced CE in northeast China (Heilongjiang), surveillance of local deer and wolves for *Echinococcus* infection should be implemented (*9*), whereas for *Ei*-induced CE occurring in northwest China (Xinjiang and Inner Mongolia), infection surveillance in camels is warranted (*10*). Furthermore, *Ee*-induced CE, prevalent in Central Asia (Kyrgyzstan) and posing a pathogenic threat to humans, necessitates surveillance of Equidae animals (horses and donkeys) in neighboring areas of China (Xinjiang).

Conflicts of interest: No conflicts of interest.

Funding: Supported by the the National Natural Science Foundation of China (Nos. 82404325, 31470488 and 32071529), and the NHC Key Laboratory of Echinococcosis Prevention and Control (Grant Number 2023WZK1002).

doi: 10.46234/ccdcw2025.147

Corresponding authors: Shuai Han, hanshuai@nipd.chinacdc.cn; Zhenghuan Wang, zhwang@bio.ecnu.edu.cn.

---

[1] National Institute of Parasitic Diseases, Chinese Center for Disease Control and Prevention; Chinese Center for Tropical Diseases Research; National Key Laboratory of Intelligent Tracking and Forecasting for Infectious Diseases; Key Laboratory on Parasite and Vector Biology, Ministry of Health; World Health Organization Collaborating Centre for Tropical Diseases; National Center for International Research on Tropical Diseases, Ministry of Science and Technology, Shanghai, China; [2] Key Laboratory of Echinococcosis Prevention and Control, National Health Commission, Lhasa City, Xizang Autonomous Region, China; [3] Chengdu Center for Disease Control and Prevention, Sichuan Province, Chengdu City, Sichuan Province, China; [4] Chinese Center for Tropical Diseases Research, School of Global Health, Shanghai Jiao Tong University School of Medicine, Shanghai, China; [5] One Health Center, Shanghai Jiao Tong University-The University of Edinburgh, Shanghai, China; [6] School of Life Science, Fudan University, Shanghai, China; [7] School of Life Sciences, East China Normal University, Shanghai, China.

Submitted: March 25, 2025
Accepted: June 17, 2025
Issued: June 27, 2025

REFERENCES

1. Wang X, Han S, Cao JP. Brief recognition history of *Echinococcus* tapeworm. In: Li J, Wang W, Mehlhorn H, editors. Echinococcus: control and elimination of *echinococcosis* with a focus on China and Europe. Cham: Springer. 2024; p. 1-13. http://dx.doi.org/10.1007/978-3-031-54479-8_1.
2. Fu MH, Wang X, Han S, Guan YY, Bergquist R, Wu WP. Advances in research on echinococcoses epidemiology in China. Acta Trop 2021;219:105921. https://doi.org/10.1016/j.actatropica.2021.105921.
3. Shams M, Khazaei S, Naserifar R, Shariatzadeh SA, Anvari D, Montazeri F, et al. Global distribution of *Echinococcus granulosus* genotypes in domestic and wild canids: a systematic review and meta-analysis. Parasitology 2022;149(9):1147 – 59. https://doi.org/10.1017/S0031182022000658.
4. Massolo A, Simoncini A, Romig T. The ‘bridge effect’ by intermediate hosts may explain differential distributions of *Echinococcus* species. Trends Parasitol 2022;38(7):501 – 12. https://doi.org/10.1016/j.pt.2022.04.003.
5. Romig T, Wassermann M. *Echinococcus* species in wildlife. Int J Parasitol Parasites Wildl 2024;23:100913. https://doi.org/10.1016/j.ijppaw.2024.100913.
6. Wang X, Kui Y, Xue CZ, Wang Q, Zheng CJ, Zhao JS, et al. Past, present and future epidemiology of echinococcosis in China based on nationwide surveillance data 2004-2022. J Infect 2025;90(3):106445. https://doi.org/10.1016/j.jinf.2025.106445.
7. Hogea MO, Ciomaga BF, Muntean MM, Muntean AA, Popa MI, Popa GL. Cystic echinococcosis in the early 2020s: a review. Trop Med Infect Dis 2024;9(2):36. https://doi.org/10.3390/tropicalmed9020036.
8. Wang X, Zhu AY, Cai HY, Liu BX, Xie G, Jiang R, et al. The pathology, phylogeny, and epidemiology of *Echinococcus ortleppi* (G5 genotype): a new case report of echinococcosis in China. Infect Dis Poverty 2021;10(1):130. https://doi.org/10.1186/s40249-021-00907-3.
9. Yang D, Zhang TM, Zeng ZL, Zhao W, Zhang WZ, Liu AQ. The first report of human-derived G10 genotype of *Echinococcus canadensis* in China and possible sources and routes of transmission. Parasitol Int 2015;64(5):330 – 3. https://doi.org/10.1016/j.parint.2015.05.001.
10. Bart JM, Abdukader M, Zhang YL, Lin RY, Wang YH, Nakao M, et al. Genotyping of human cystic echinococcosis in Xinjiang, PR China. Parasitology 2006;133(Pt 5):571-9. http://dx.doi.org/10.1017/S0031182006000734.

SUPPLEMENTARY MATERIAL

List of Countries and Regions where *Echinococcus* species have been Reported

Echinococcus granulosus:

Afghanistan, Albania, Algeria, Argentina, Armenia, Australia, Austria, Azerbaijan, Bahrain, Bangladesh, Belgium, Bhutan, Bolivia, Bosnia and Herzegovina, Brazil, Bulgaria, Chile, China, Croatia, Cyprus, Czech Republic, Egypt, Estonia, Ethiopia, Finland, France, Georgia, Germany, Greece, Hungary, Iceland, India, Indonesia, Iran, Iraq, Ireland, Israel, Italy, Jordan, Kazakhstan, Kenya, Kosovo, Kuwait, Kyrgyzstan, Latvia, Lebanon, Libya, Lithuania, Luxembourg, North Macedonia, Malta, Mauritania, Mexico, Moldova, Mongolia, Montenegro, Morocco, Namibia, Nepal, Nigeria, Norway, Oman, Pakistan, Palestine, Peru, Poland, Portugal, Qatar, Romania, Russia, Saudi Arabia, Serbia, Slovakia, Slovenia, South Africa, Spain, Sudan, Sweden, Switzerland, Syria, Tajikistan, Tanzania, Tunisia, Turkey, Turkmenistan, Uganda, UK, Ukraine, Uruguay, Uzbekistan, Vietnam, Yemen.

E. multilocularis:

Afghanistan, Albania, Armenia, Austria, Azerbaijan, Belgium, Bosnia and Herzegovina, Bulgaria, Canada, China, Croatia, Cyprus, Czech Republic, Denmark, Estonia, Finland, France, Georgia, Germany, Greece, Hungary, Iran, Iraq, Ireland, Italy, Japan, Kazakhstan, Kosovo, Kyrgyzstan, Latvia, Liechtenstein, Lithuania, Luxembourg, North Macedonia, Malta, Mongolia, Montenegro, Netherlands, Norway, Pakistan, Poland, Portugal, Romania, Russia, Serbia, Slovakia, Slovenia, South Korea, Spain, Sweden, Switzerland, Tajikistan, Turkey, Turkmenistan, UK, Ukraine, USA, Uzbekistan.

E. intermedius:

Afghanistan, Algeria, Argentina, Austria, Bolivia, Brazil, Cape Verde, Chile, China, Ecuador, Egypt, Ethiopia, France, Ghana, Greece, Hungary, India, Iran, Italy, Kazakhstan, Kenya, Libya, Lithuania, Mali, Mauritania, Mexico, Moldova, Mongolia, Namibia, Nigeria, Oman, Pakistan, Peru, Poland, Portugal, Romania, Russia, Saudi Arabia, Serbia, Slovakia, Slovenia, Somalia, South Africa, Spain, Sudan, Tanzania, Tunisia, Turkey, Uganda, Ukraine, Zambia.

E. ortleppi:

Argentina, Bhutan, Bolivia, Bosnia and Herzegovina, Brazil, Chile, China, Egypt, Ethiopia, France, Germany, India, Iran, Italy, Kenya, Mexico, Mozambique, Namibia, Nepal, Netherlands, Pakistan, Poland, Portugal, Saudi Arabia, Serbia, South Africa, South Sudan, Sudan, Switzerland, Tanzania, Turkey, UK, Uruguay, Vietnam, Zambia.

E. equinus:

Canada, Chile, Egypt, Ethiopia, Germany, Ireland, Italy, Kenya, Kyrgyzstan, Namibia, Pakistan, South Africa, Spain, Tunisia, Turkey, UK, Uzbekistan.

E. canadensis:

Canada, China, Estonia, Finland, Latvia, Mongolia, Poland, Russia, Sweden, USA.

E. vogeli:

Argentina, Bolivia, Brazil, Colombia, Ecuador, Guyana, Panama, Peru, Suriname, Venezuela.

E. oligarthra:

Argentina, Brazil, Colombia, Costa Rica, Mexico, Panama, Suriname, Venezuela.

E. felidis:

Kenya, Namibia, South Africa, Uganda, Zambia.

E. shiquicus:

China.

Preplanned Studies

Drug Resistance of Imported *P. falciparum* and *P. vivax* Isolates — China, 2021–2023

He Yan[1]; Yan Deng[2]; Siqi Wang[1]; Jianhai Yin[1]; Zhigui Xia[1,#]; Jianping Cao[1,3,#]

Summary

What is already known about this topic?

Artemisinin-based combination therapies (ACTs) remain the first-line treatment for uncomplicated malaria caused by *P. falciparum*, while chloroquine (CQ) serves as the primary treatment for *P. vivax*. However, the global spread of antimalarial drug resistance has become an increasing concern over time.

What is added by this report?

The integrated drug efficacy studies (iDES) demonstrated that artesunate (AS) plus dihydroartemisinin-piperaquine (DHA-PPQ) and chloroquine (CQ) remain effective first-line treatments for *P. falciparum* and *P. vivax* malaria, respectively. However, the occurrence of late treatment failure (LTF) and day 3 (D3) parasite positivity following treatment, suggests decreasing therapeutic efficacy. Molecular surveillance of *P. falciparum* resistance revealed novel mutation sites in *pfK13* (S459T, N499T, A578S, and V692L) in addition to the previously reported F446I, P574L, and C580Y mutations. Concurrently, the difference in mutation patterns between *pfcrt* and *pfmdr1* was significant ($P<0.01$), with the Y184F locus of the multidrug resistance gene *pfmdr1* showing the highest mutation frequency at 40.5% of cases.

What are the implications for public health practice?

The iDES and molecular surveillance of antimalarial drug resistance indicated decreasing sensitivity to current first-line treatments. Continued surveillance of antimalarial drug resistance is vital for early warning and appropriate response to the spread of resistant parasites.

ABSTRACT

Introduction: Malaria remains the leading cause of infectious disease-related morbidity and mortality worldwide. ACTs continue to be the first-line treatment for uncomplicated malaria caused by *P. falciparum*. However, the global spread of antimalarial drug resistance, particularly artemisinin resistance, has become an increasing concern over time.

Methods: Therapeutic efficacy was evaluated following the World Health Organization's guidelines for iDES. This study assessed adequate clinical and parasitological response (ACPR) and parasitemia on day 3 of treatment. Molecular surveillance of resistance-associated genes, including *pfk13*, *pfcrt*, and *pfmdr1*, was conducted on collected *P. falciparum* isolates.

Results: The iDES of AS plus DHA-PPQ was implemented in 2023, while CQ efficacy was monitored from 2021 to 2023. Late parasitological failure (LCF) for DHA-PPQ was detected in 1 of 26 *P. falciparum* cases in 2023, and in 1 of 26 and 1 of 90 *P. vivax* cases for CQ in 2022 and 2023, respectively. The corresponding ACPR rates were 96.2%, 100%, 96.2%, and 98.8%. The average positive parasitemia rate on day 3 post-treatment was 21.8%. Molecular polymorphism analysis revealed 9 nonsynonymous mutation haplotypes in the *pfk13* gene, while 97.7% of samples presented the wild-type genotype. For the chloroquine resistance-associated *pfcrt* gene, 2 mutant haplotypes, 'CVIET' and 'SVMNT', were detected with frequencies of 16.7% (70/418) and 0.5% (2/418), respectively, while the wild-type haplotype 'CVMNK' predominated at 82.8% (346/418). In the *pfmdr1* gene, 5 nonsynonymous point mutations and 8 haplotypes were identified. The Y184F mutation showed the highest prevalence at 40.5% (170/420). The 7 mutant haplotypes detected were V65L (0.2%, 1/420), N86Y (1.9%, 8/420), F408V (0.9%, 4/420), D1246Y (0.5%, 2/420), V65L/Y184F (0.2%, 1/420), N86Y/Y184F (0.7%, 3/420), and Y184F (39.8%, 167/420).

Conclusion: The antimalarial drug efficacy studies conducted for AS plus DHA-PPQ and CQ demonstrated that these treatments remain effective. However, the occurrence of LCF cases and persistent parasitemia on day 3 indicate decreasing sensitivity of these first-line drugs for treating *P. falciparum* and *P.*

vivax, respectively. Therefore, continuous iDES and molecular surveillance of antimalarial drugs must be enhanced to provide early warning and guide appropriate responses to the spread of antimalarial drug resistance.

Malaria remains a significant global health challenge affecting 84 endemic countries, with an estimated 257 million infections and 597,000 deaths reported in 2023 (*1*). China achieved malaria-free certification from the World Health Organization (WHO) on June 30, 2021, following decades of elimination efforts (*2*). However, the increasing influx of *Plasmodium*-infected individuals from malaria-endemic regions, particularly sub-Saharan Africa and Southeast Asia, poses a substantial challenge to China's post-elimination phase (*3–4*). Systematic monitoring of antimalarial drug efficacy aims to establish a centralized drug resistance database for imported strains, providing actionable intelligence for source countries and aligning with the WHO's "High Burden to High Impact" strategy by informing region-specific antimalarial protocols (*5*).

Antimalarial drugs, especially artemisinin derivatives, are the most widely used treatments globally (*6*). Although China has reported no indigenous malaria cases since 2017, the challenges in preventing and controlling imported malaria have intensified, particularly with the emergence and spread of drug-resistant strains (*6–7*). While the treatment efficacy survey (TES) remains the gold standard for evaluating antimalarial drug efficacy, iDES are more appropriate in low-endemic or malaria elimination settings (*5*,*8*). This study employed an iDES protocol combined with analysis of drug resistance-associated molecular markers (*pfk13*, *pfcrt*, and *pfmdr1*) to monitor and evaluate the therapeutic efficacy of ACTs and CQ from 2021–2023, thereby providing baseline data to inform antimalarial drug policies.

The iDES and detection of drug resistance-associated molecular markers were performed according to previously described protocols (*8–9*). All experiments were conducted within the provincial malaria diagnostic laboratory network, with data uploaded to the National Information System for Parasitic Disease Prevention and Control. iDES was implemented to evaluate ACTs for *P. falciparum* treatment and CQ for *P. vivax* treatment in Yunnan Province. Patients with confirmed *P. falciparum* or *P. vivax* infection, excluding those with severe malaria, were followed from the first day of treatment (Day 0, D0) through D1-3, D7, D14, D21, D28, D35, and D42. Treatment outcomes were classified according to WHO guidelines for therapeutic efficacy monitoring as early treatment failure (ETF), LCF, late parasitological failure (LPF), or ACPR (*5*).

All malaria species were confirmed via PCR and microscopy. Molecular polymorphisms of *PfK13*, *Pfcrt*, and *Pfmdr1* genes were detected and sequenced from imported malaria cases from 2021–2023. The chi-square test was used to evaluate differences in the distribution of drug resistance-associated gene polymorphisms, and data analysis was performed using GraphPad Prism 8.0 software.

A total of 174 cases of *P. falciparum* and *P. vivax* malaria were monitored for clinical efficacy through the iDES protocol (Table 1). In 2023, 26 cases of *Pf* malaria treated with AS combined with DHA-PPQ were included in the iDES follow-up. Among these, 25 patients achieved ACPR, while one patient tested positive for parasitemia on day 35, which was classified as late treatment failure. Additionally, 8 patients (30.8%, 8/26) exhibited persistent parasitemia on day 3 of treatment.

For *Pv* malaria, the treatment regimen consisted of chloroquine and primaquine. From 2021 to 2023, a total of 148 *Pv* malaria cases were followed up. In 2021, all 32 patients achieved ACPR, with only 1 patient showing parasitemia on day 3. In 2022, 4 out of 26 patients were lost to follow-up, 1 patient was classified as having late treatment failure (LTF), and 6 patients (27.2%, 6/22) demonstrated persistent parasitemia on day 3. In 2023, among the 90 cases targeted for follow-up, 8 were lost to follow-up, 1 case was identified as LTF, and 23 cases (28.0%, 23/82) presented with parasitemia on day 3.

A total of 451 cases of *P. falciparum* malaria were subjected to molecular testing for drug-resistance markers (Table 2). Of these, 442 samples were successfully sequenced for the *pfk13* gene. 9 distinct point mutations were identified at the following loci: P441T, F446I, S459T, C469F, N499T, P574L, A578S, C580Y, and V692L (where the left side represents the wild-type allele and the right side represents the mutant allele). All the detected *pfk13* mutations were single-point mutations. A total of 418 samples were successfully genotyped for the CQ resistance-associated *pfcrt* gene, with a focus on mutations at codons 72–76. 3 genotypes were identified (Table 3): the wild-type CVMNK and the

TABLE 1. Treatment outcomes for DHA-PPQ and CQ by iDES.

Item	AS+DHA-PPQ	CQ			Total
	2023	2021	2022	2023	
ETF	0	0	0	0	0
LCF	1	0	1	1	3
LPF	1	0	1	1	3
LFU	0	0	4	8	12
ACPR (*n*, %)	25 (96.2)	32 (100.0)	21 (96.2)	81 (98.8)	NA
No. of Day 3(+) (*n*, %)	8 (30.8)	1 (3.1)	6 (27.2)	23 (28.0)	38 (21.8)
Total	26	32	26	90	174

Abbreviation: iDES=integrated drug efficacy studies; ETF=early treatment failure; LCF=late clinical failure; LPF=late parasitological failure; ACPR=adequate clinical and parasitological response; LFU=lost to follow-up; AS=Artesunate; DHA-PPQ=dihydroartemisinin–piperaquine; CQ=chloroquine; NA=not applicable.

TABLE 2. Polymorphisms of SNPs in genes associated with anti-malarial drug resistance, 2021–2023.

Gene	No. of detected samples	Loci	Wild type	Mutant type	Variant genotype	No. of mutant samples	Mutant proportion (%)
Pfk13	442	441	cca	aca	P441T	2	0.5
		446	ttt	att	F446I	1	0.2
		459	tcg	acg	S459T	1	0.2
		469	tgc	ttc	C469F	1	0.2
		499	aac	acc	N499T	1	0.2
		574	cct	ctt	P574L	1	0.2
		578	gct	tct	A578S	1	0.2
		580	tgt	tat	C580Y	1	0.2
		692	gtt	ctt	V692L	1	0.2
Pfcrt	418	72	tgt	agt	C72S	2	0.5
		74	atg	aat	M74I	70	16.7
		75	aat	gaa	N75E	70	16.7
		76	aaa	aca	K76T	72	17.2
pfmdr1	420	65	ctg	tct	V65L	2	0.5
		86	aat	tat	N86Y	11	2.6
		184	tat	ttt	Y184F	170	40.5
		408	ttt	gtt	F408V	4	1.0
		1,246	gat	tat	D1246Y	2	0.5

Abbreviation: SNPs=single nucleotide polymorphisms; No.=Number.

mutant types CVIET and SVMNT. The most frequent mutation was K76T, which was detected in 72 samples. The SVMNT haplotype was observed in 2 samples, both originating from Southeast Asia (one from Indonesia and one from Bangladesh). In total, 420 samples were analyzed for *pfmdr1* point mutations, revealing 5 mutation types and 7 mutant haplotypes. The most frequent mutation was Y184F, which was detected in 170 samples (40.5%), followed by N86Y (2.6%, 11/420). The 7 haplotypes included 2 novel combinations: l65f184 and $Y_{86}F_{148}$ (Table 3).

DISCUSSION

Regarding the clinical efficacy monitoring of AS plus DHA-PPQ, although this work was only conducted in 2023 due to policy requirements, the detection of parasitemia on day 3 (D3+) in 8 out of 26 cases clearly indicates prolonged parasite clearance time for ACTs, demonstrating decreased sensitivity to these drugs. Additionally, 1 patient tested positive for parasitemia by blood smear microscopy on day 35 (D35) posttreatment, which was classified as late treatment

TABLE 3. Source of importation and haplotypes distribution of *pfcrt* and *pfmdr1*.

Gene	Regions or countries (*n*, proportion%)	Haplotype	No. of genotypes	Proportion (%)
pfcrt (*n*=418)	Southeast Asia (*n*=5, 1.2)	$S_{72}V_{73}M_{74}N_{75}T_{76}$	2	0.5
	Eastern Africa (*n*=72, 17.2)	$C_{72}V_{73}I_{74}E_{75}T_{76}$	70	16.7
	Western Africa (*n*=148, 35.4)	$C_{72}V_{73}M_{74}N_{75}K_{76}$ (wild type)	346	82.8
	Central Africa (*n*=191, 45.7)			
	other regions (*n*=2, 0.4)			
pfmdr1 (*n*=420)	Southeast Asia (*n*=5, 1.2)	L_{65}	1	0.2
	Eastern Africa (*n*=72, 17.1)	$L_{65}F_{184}$	1	0.2
	Western Africa (*n*=148, 35.2)	Y_{86}	8	1.9
	Central Africa (*n*=193, 46.0)	$Y_{86}F_{184}$	3	0.7
		V_{408}	4	0.9
	Other regions (*n*=2, 0.4)	Y_{1246}	2	0.5
		F_{184}	167	39.8
		Wild type	234	55.7

Abbreviation: No.=Number.

failure. Similarly, in the follow-up of *P. vivax* cases, the first parasite clearance time also showed an increasing trend over time. When excluding patients lost to follow-up, late treatment failure was observed each year. These phenomena suggest decreasing sensitivity of ACTs and CQ as first-line treatments for *P. falciparum* and *P. vivax* malaria, respectively. These findings further underscore the urgency and importance of the World Health Organization's efforts to contain the spread of artemisinin resistance.

In the molecular detection of *pfk13*, this study identified K189T as a relatively dominant mutation site; however, it is not listed in Table 2 since it is not localized in the BTB/POZ region of the Kelch protein, the function of which remains unclear (*10*–*11*). This mutation was predominantly distributed in West African countries (such as Côte d'Ivoire, Nigeria, the Democratic Republic of the Congo, and Cameroon), with 1 case each detected in North Africa and East Africa (from Zambia and Algeria, respectively). Other newly detected mutation sites including S459T, N499T, A578S, and V692L were reported for the first time (*10*). However, it remains unclear whether these novel mutations will become fixed over time. For the *pfcrt* gene, the K76T point mutation is highly associated with CQ resistance. Nevertheless, the proportion of the wild-type genotype exceeded 82%, and compared with the variation in *pfmdr1*, the difference between *pfcrt* and *pfmdr1* was statistically significant by Chi-square test (P<0.01), supporting the observation that sensitivity to CQ is gradually recovering following the withdrawal of CQ (*12*–*13*). Furthermore, detection of *pfmdr1* gene mutations revealed that Y184F was the most frequently mutated site, indicating its potential association with multidrug resistance, particularly in the context of resistance to ACTs and their partner drugs.

In conclusion, this study employed two approaches — iDES and drug resistance-associated molecular detection — to evaluate the efficacy of antimalarial drugs. As the current gold standard for clinical drug efficacy evaluation, iDES requires sustained and substantial investments in human and material resources. Based on the initial results presented in this study, future efforts must leverage the comprehensive parasitic disease prevention and management information system to achieve two critical objectives: 1) expanding the clinical follow-up sample size and 2) ensuring nationwide coverage of imported malaria cases. These steps will enable more objective and timely assessments of antimalarial drug efficacy in real-time settings, thereby mitigating the risk of further drug resistance dissemination.

Acknowledgments: The staff involved in field investigations and to provincial CDC personnel participating in the national antimalarial drug resistance network. We also thank all malaria patients who were recruited for the iDES.

Conflicts of interest: No conflicts of interest.

Funding: Supported by Young Scholar Science Foundation of China CDC (grant number 2024A105); Three-Year Initiative Plan for Strengthening Public Health System Construction in Shanghai (2023-2025) Key Discipline Project [grant number GWVI-11.1-12 to JC].

doi: 10.46234/ccdcw2025.149

[#] Corresponding authors: Jianping Cao, caojp@chinacdc.cn; Zhigui Xia, xiazg@nipd.chinacdc.cn.

---

[1] National Key Laboratory of Intelligent Tracking and Forecasting for Infectious Diseases, NHC Key Laboratory of Parasite and Vector Biology, World Health Organization Collaborating Centre for Tropical Diseases, National Center for International Research on Tropical Diseases; National Institute of Parasitic Diseases (Chinese Center for Tropical Diseases Research), Chinese Center for Disease Control and Prevention, Shanghai, China; [2] Yunnan Provincial Key Laboratory of Vector-borne Diseases Control and Research; Yunnan Provincial Center of Malaria Research; Yunnan Institute of Parasitic Diseases Innovative Team of Key Techniques for Vector Borne Disease Control and Prevention; Yunan International Joint Laboratory of Tropical Infectious Diseases, Kunming, Yunnan, China; [3] The School of Global Health, Chinese Center for Tropical Diseases Research, Shanghai Jiao Tong University School of Medicine, Shanghai, China.

Submitted: April 27, 2025
Accepted: June 16, 2025
Issued: June 27, 2025

REFERENCES

1. WHO. World malaria report 2024. Geneva: World Health Organization; 2024. https://www.who.int/teams/global-malaria-programme/reports/world-malaria-report-2024.
2. Feng XY, Zhang L, Tu H, Xia ZG. Malaria elimination in China and sustainability concerns in the post-elimination stage. China CDC Wkly 2022;4(44):990 – 4. https://doi.org/10.46234/ccdcw2022.201.
3. Feng XY, Feng J, Zhang L, Tu H, Xia ZG. Vector control in China, from malaria endemic to elimination and challenges ahead. Infect Dis Poverty 2022;11(1):54. https://doi.org/10.1186/s40249-022-00971-3.
4. Yin JH, Li M, Yan H, Zhou SS, Xia ZG. Laboratory diagnosis for malaria in the elimination phase in China: efforts and challenges. Front Med 2022;16(1):10 – 6. https://doi.org/10.1007/s11684-021-0889-7.
5. WHO. Methods for surveillance of antimalarial drug efficacy. Geneva: World Health Organization; 2009. https://www.who.int/publications/i/item/9789241597531.
6. World Health Organization. Global malaria programme: WHO guidelines for malaria. 2024. https://www.who.int/publications/i/item//guidelines-for-malaria.
7. Zhang L, Feng J, Zhang SS, Xia ZG, Zhou SS. The progress of national malaria elimination and epidemiological characteristics of malaria in China in 2017. Chin J Parasitol Parasit Dis 2018;36(3):201-9. https://d.wanfangdata.com.cn/periodical/ChtQZXJpb2RpY2FsQ0hJMjAyNTA2MTcxNjU3NTMSFnpnanNjeHlqc2NienoyMDE4MDMwMDEaCHhyYjhmaTM2. (In Chinese).
8. Huang F, Liu H, Yan H, Zhou SS, Xia ZG. Antimalarial drug resistance surveillance in China, 2016-2020. China CDC Wkly 2021;3(17):366 – 71. https://doi.org/10.46234/ccdcw2021.099.
9. WHO. Malaria surveillance, monitoring & evaluation: a reference manual. Geneva: World Health Organization; 2018. https://www.who.int/publications/i/item/9789241565578.
10. WHO. Artemisinin resistance and artemisinin-based combination therapy efficacy. Geneva: World Health Organization; 2018. https://iris.who.int/handle/10665/274362.
11. Ariey F, Witkowski B, Amaratunga C, Beghain J, Langlois AC, Khim N, et al. A molecular marker of artemisinin-resistant *Plasmodium falciparum* malaria. Nature 2014;505(7481):50 – 5. https://doi.org/10.1038/nature12876.
12. Mulenga MC, Sitali L, Ciubotariu II, Hawela MB, Hamainza B, Chipeta J, et al. Decreased prevalence of the *Plasmodium falciparum Pfcrt* K76T and *Pfmdr1* and N86Y mutations post-chloroquine treatment withdrawal in Katete District, Eastern Zambia. Malar J 2021;20(1):329. https://doi.org/10.1186/s12936-021-03859-z.
13. de Abreu-Fernandes R, Almeida-de-Oliveira NK, Gama BE, Gomes LR, De Lavigne Mello AR, de Queiroz LT, et al. *Plasmodium falciparum* Chloroquine-*pfcrt* resistant haplotypes in Brazilian endemic areas four decades after CQ withdrawn. Pathogens 2023;12(5):731. https://doi.org/10.3390/pathogens12050731.

Reviews

Tick-Borne Infectious Diseases in China, 2003–2023

Yinshan Zhu[1,2]; Tianxiang Jiang[1,2]; Zhishan Sun[1,2]; Jingxian Yin[1,2]; Hanqing Zhao[1,2];
Xiaonong Zhou[1,#]; Kokouvi Kassegne[1,#]

ABSTRACT

Tick-borne diseases (TBDs) pose a substantial threat to global public health, including China. This article systematically reviews the epidemiology of TBDs in Chinese mainland between 2003 and 2023. We retrieved and analyzed the incidence and distribution of notable bacterial, viral, and parasitic TBDs in China, and discussed their clinical characteristics, diagnostic approaches, and vectors. Severe fever with thrombocytopenia syndrome is the leading TBD in China, with cases rapidly increasing since its first report in 2009, and a high case fatality rate of 5%–33% in patients with severe disease. Other TBDs reported in China include spotted fever group rickettsiosis, human granulocytic anaplasmosis, Lyme borreliosis, babesiosis, and tick-borne encephalitis. Infections with emerging tick-borne pathogens, such as Yezo virus and Beiji nairovirus, have appeared very recently. Although evidence of human infection with Crimean-Congo hemorrhagic fever virus, *Francisella tularensis*, and *Bartonella* is currently unavailable, continuous monitoring of these pathogens remains necessary. This study enhances our understanding of TBDs, provides guidance for public health decision-making regarding important bacterial, viral, and parasitic TBDs, and offers new opportunities for TBD research in China.

Tick-borne diseases (hereafter referred to as TBDs), which are transmitted through ticks as vectors, are characterized by their high infectivity and wide transmission range. Recent years have witnessed a notable increase in the global incidence of these diseases (*1*–*2*), along with rising cases of coinfections with multiple tick-borne pathogens (*3*–*4*). These diseases pose serious health risks and economic burdens to both humans and animals worldwide, underscoring the critical importance of research in this field. Ongoing processes of globalization, climate change, and increased human-animal interactions have further accelerated the global spread of TBDs, leading to the emergence of new diseases (*5*–*6*). China's complex terrain, combined with diverse tick species and pathogens, presents a major public health challenge. Urbanization and afforestation projects complicate the distribution of ticks and pathogens, creating significant obstacles for disease prevention and control efforts in the country (*7*). Despite the diversity and complex distribution of tick species in China, the health threats posed by TBDs are often underestimated, hampering current prevention and control initiatives. By analyzing research literature, we can develop a better understanding of the characteristics of various TBDs in China to improve preventive measures.

METHODS

Search Strategy

A systematic literature review was conducted using Embase, PubMed, Scopus, and the Web of Science Core Collection. The search terms included 'Tick-borne diseases' OR 'Lyme borreliosis' OR 'Tick-borne encephalitis' OR 'Q fever' OR 'Babesiosis' OR 'Crimean-Congo haemorrhagic fever' OR 'African swine fever' OR 'Tularemia' OR 'Kyasanur forest disease' OR 'Colorado tick fever' OR 'Ehrlichiosis' OR 'Anaplasmosis' OR 'Rocky Mountain spotted fever' OR 'Southern tick-associated rash illness' OR 'Tick-borne relapsing fever' OR 'Pacific coast tick fever' OR 'Omsk haemorrhagic fever' OR 'Rickettsiosis' OR 'Spotted fever group rickettsiosis' OR 'Novel bunyavirus infection' OR 'Piroplasmosis' OR 'Oriental spotted fever' OR 'Relapsing fever borrelioses' OR 'Powassan disease' OR 'Powassan encephalitis' OR 'Imported tick-borne spotted fever' OR 'North-Asia spotted fever' OR 'African tick bite fever'. As *China CDC Weekly* is an international peer-reviewed journal that ensures research reproducibility, this study included only English-language publications. The review was limited to research articles published between 2003 and 2023, excluding reviews, case reports, commentaries, interviews, letters, and editorials. Mite-, flea-, and louse-borne diseases, such as Tsutsugamushi, murine rickettsiosis, and infections caused by *Rickettsia felis*, *Rickettsia akari*, and *Rickettsia prowazekii*, were excluded. After removing duplicate articles using EndNote and Excel, only studies related to TBDs were included.

Data Processing

We systematically processed data on TBDs from the articles that met the inclusion criteria. These data include geographical origins of cases, incidence and distribution, clinical characteristics, diagnostic methods, and tick vectors.

RESULTS

Literature Screening

A total of 3,483 articles were initially retrieved from Embase, PubMed, the Web of Science Core Collection, and Scopus. After screening, 67 relevant articles specifically related to TBDs were retained for inclusion in the study. The detailed screening process is illustrated in Figure 1.

Analysis of these 67 articles revealed temporal trends in TBD cases (Figure 2A). The number of patients with severe fever with thrombocytopenia syndrome (SFTS) gradually increased in 2020, peaked in 2021, and then progressively declined in subsequent years. A summary of articles and cases related to various TBDs (Figure 2B) showed that 43% of the articles focused on SFTS, 18% on spotted fever group rickettsiosis (SFGR), and 14% on human granulocytic anaplasmosis (HGA). This finding indicates a shift in research attention toward TBDs in China, with SFTS attracting significant interest among researchers. Furthermore, SFTS accounted for the greatest number of cases, representing 66% (10,080/15,261) of the total TBD cases reported in the country. This underscores SFTS as the most prominent health concern among TBDs in China.

Distribution of TBDs in China

We assessed the geographical distribution of TBD cases across Chinese mainland (Figure 2C). This

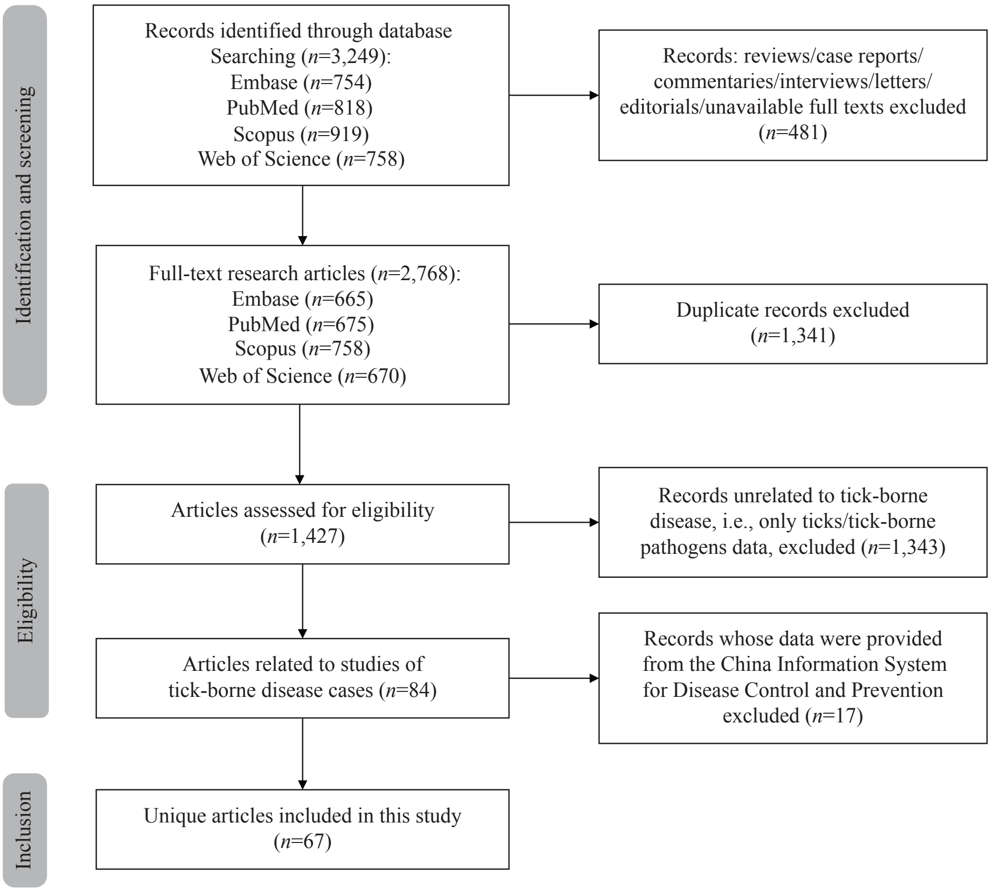

FIGURE 1. Flowchart illustrating the search and screening process for articles on tick-borne diseases in China.

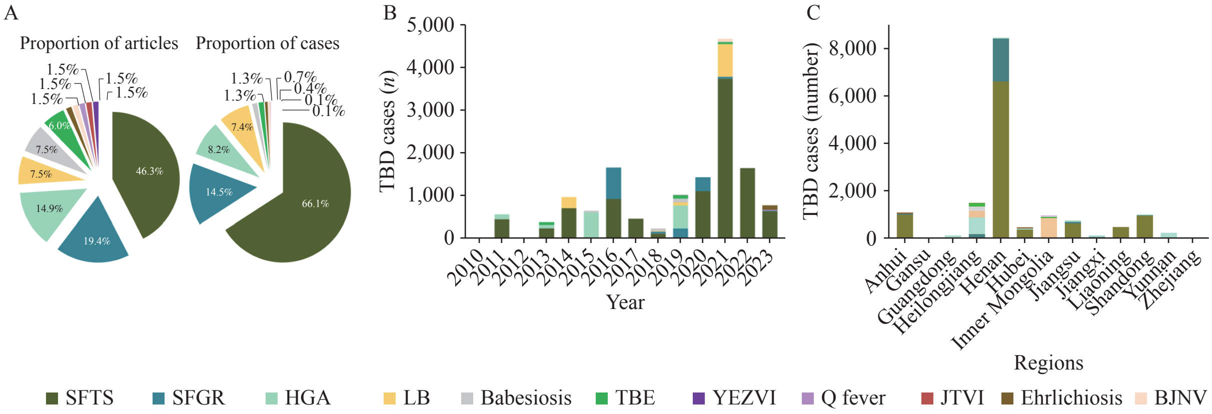

FIGURE 2. Distribution of articles and yearly cases of tick-borne diseases in China, 2003–2023. (A) The proportion of articles and cases related to tick-borne diseases; (B) Number of cases per tick-borne disease across the years; (C) Incidence of tick-borne diseases reported across Chinese mainland.

Abbreviation: SFTS=severe fever with thrombocytopenia syndrome; SFGR=spotted fever group rickettsiosis; HGA=human granulocytic anaplasmosis; LB=Lyme borreliosis; TBE=tick-borne encephalitis; YEZVI=Yezo virus infection; JTVI=Jingmen tick virus infection; BJNV=Beiji nairovirus.

analysis revealed a concentration of TBD cases primarily in provincial-level administrative divisions (PLADs) such as Henan, Heilongjiang, Anhui, Shandong, Inner Mongolia, and Jiangsu. These findings align with the known distribution of ticks and tick-borne pathogens (*7*). Additionally, SFTS alone accounted for 10,080 of the 15,261 total TBD cases reported in China, followed by SFGR and HGA, which accounted for 2,212 and 1,257 cases, respectively. Notably, 61.2% (6,611/10,800) of SFTS cases and 81.8% (1,810/2,212) of SFGR cases were reported in Henan Province, 37.9% (477/1,257) of HGA cases were reported in Heilongjiang Province, and 68.5% (771/1,126) of Lyme borreliosis (LB) cases and 74.9% (149/199) of tick-borne encephalitis (TBE) cases were reported in Inner Mongolia Autonomous Region.

A comprehensive categorization of TBDs into viral, bacterial, and parasitic types is presented in Table 1. The clinical characteristics, diagnostic methods, and tick species for these diseases are summarized. In China, *Haemaphysalis longicornis*, *Ixodes persulcatus*, and *Haemaphysalis yeni* serve as the primary vectors for numerous tick-borne pathogens. This prevalence might be attributed to the favorable environmental conditions in China that are conducive to the proliferation of these particular tick species (*7*).

Major Tick-borne Diseases in China

SFTS SFTS is a recently identified infectious disease that originated in China and is caused by a novel bunyavirus (*65*). In China, SFTSV has been detected in *Haemaphysalis longicornis* ticks collected from livestock in areas where SFTS patients reside, establishing this species as the primary transmission vector (*66*). SFTS cases in China are primarily concentrated in Liaoning Province in northeastern China; Shandong Province along the eastern coast; Jiangsu and Zhejiang provinces in eastern China; and Henan, Hubei, and Anhui provinces in central China (*7*). According to this study, a total of 10,080 SFTS cases have been identified in China. The characteristic clinical manifestations include acute fever, fatigue, thrombocytopenia, leukopenia, and gastrointestinal symptoms such as nausea, vomiting, and diarrhea. In severe cases, multiple organ dysfunction may occur (*10*). Currently, no specific treatment or vaccine is available for this disease, making effective prevention measures crucial in endemic areas (*66*).

SFGR SFGR is a zoonosis caused by bacteria of the genus *Rickettsia* and is transmitted primarily by arthropod vectors, particularly ticks (*67*). This study identified 2,212 SFGR cases reported in China. The clinical presentation typically includes fever, rash, and other characteristic features such as eschars and lymphadenopathy (*68*). Early diagnosis and treatment are essential, with antibiotics commonly used to alleviate symptoms and prevent disease progression. Preventive measures include avoiding tick bites, practicing good personal hygiene, and maintaining clean living environments. Our analysis revealed that *Haemaphysalis yeni* and *H. longicornis* serve as the primary vectors for SFGR in China.

HGA HGA is an infectious bacterial disease caused

TABLE 1. Characteristics of TBDs reported in China, 2003–2023.

Category	TBD	Pathogen	Clinical symptom	Biochemical indicator	Identification method	Tick species	Citation
Viral diseases	SFTS	Severe fever with thrombocytopenia syndrome virus	Fever, anorexia, headache, muscular soreness, diarrhea, dizziness, ecchymosis, arthrodynia, central nervous system symptoms	Thrombocytopenia, leukocytopenia, elevated aminotransferase levels, elevated lactate dehydrogenase levels, proteinuria, hematuresis	RT-PCR	*H. longicornis*	(*8–41*)
	TBE	Tick-borne encephalitis virus	Fever, headache, central nervous system symptoms	Increased white blood cell count, neutrophilic leukocytosis, elevated aminotransferase levels	PCR	NA	
	Jingmen tick virus infection	Jingmen tick virus	Fever, headache, myodynia, pruritus, eschar, lymphadenectasis	Elevated aminotransferase levels, neutropenia	RT-PCR	*I. persulcatus*	
	Yezo virus infection	Yezo virus	Fever, headache, dizziness, diminution of vision, chest distress, breathe hard, arthrodynia	Lymphocytopenia, neutrophilic leukocytosis, elevated aminotransferase levels	RT-PCR	*I. persulcatus*	
	Beiji nairovirus infection	Beiji nairovirus	Fever, headache, redness and swollen, pruritus, depression, coma, fatigue, myalgia, arthralgia, poor appetite, skin rashes, petechiae	Thrombocytosis, leukocytosis, elevated level of high sensitivity C-reactive protein, elevated aminotransferase levels, elevated lactate dehydrogenase levels	PCR	NA	
Bacterial diseases	HGA	*Anaplasma phagocytophilum*	Fever, headache, dizziness, weakness, malaise, anorexia, nausea, chills, cough, abdominal pain, myalgia, ecchymosis, rash, lymphadenectasis	Leukocytopenia, thrombocytopenia, elevated aminotransferase levels, elevated lactate dehydrogenase levels	PCR, IFA	*H. longicornis*	(*42–60*)
	SFGR	*Rickettsia rickettsii*	Fever, headache, asitia, weakness, cough, dizziness, rash, eschar, lymphadenectasis	Thrombocytopenia, leukocytopenia, elevated aminotransferase levels	PCR, IFA	*H. yeni,H. longicornis*	
	LB	*Borrelia burgdorferi*	Erythema migrans, fever, headache, weak, naupathia, arthrodynia, asitia, lymphadenectasis, erythra, eschar	Elevated aminotransferase levels, thrombocytopenia, leukocytosis	PCR	NA	
	Ehrlichiosis	*Ehrlichia* spp.	Fever, rash, asthenia, anorexia, myalgia	Thrombocytopenia, leukocytopenia, elevated aminotransferase levels, increased C-reactive protein	PCR	*H. longicornis*	
	Q fever	Q fever *Rickettsia*	Fever, headache, muscular soreness, erythra, eschar	Thrombocytopenia, elevated high-sensitivity C-reactive protein levels, elevated aminotransferase levels	PCR	NA	
Parasitic diseases	Babesiosis	*Babesia* spp.	Fever, headache, dizziness, naupathia, chills, arthralgia, lymphadenectasis, flu-like symptoms	Thrombocytopenia, leukocytosis, elevated aminotransferase levels, elevated bilirubin levels	PCR	NA	(*61–64*)

Abbreviation: TBD=tick-borne disease; SFTS=severe fever with thrombocytopenia syndrome; TBE=tick-borne encephalitis; BJNV=Beiji nairovirus; HGA=human granulocytic anaplasmosis; SFGR=spotted fever group rickettsiosis; LB=Lyme borreliosis; RT-PCR=reverse transcription polymerase chain reaction; PCR=polymerase chain reaction; IFA=immunofluorescence assay; *H.=Haemaphysalis*; *I.=Ixodes*; NA=no relevant results found.

by *Anaplasma phagocytophilum* (*69*). The primary transmission route is through tick bites, with blood transfusion representing another documented mode of transmission (*70–71*). This study identified 1,257 HGA patients in China. Typical clinical manifestations include fever, headache, myalgia, fatigue, nausea, vomiting, general malaise, and thrombocytopenia with associated bleeding abnormalities (*42*). HGA cases in China are primarily concentrated in the central and southeastern regions (*72*). The Infectious Diseases Society of America (IDSA) recommends empiric treatment with doxycycline for all patients with suspected HGA (*73*). In China, *Haemaphysalis longicornis* serves as the primary vector for HGA.

LB LB is a naturally occurring epidemic disease caused by *Borrelia burgdorferi* and is transmitted primarily by ticks, particularly those in the genus *Ixodes* (*74*). Although LB is the most commonly reported tick-borne illness in the United States, China has reported fewer cases, with a total of 1,126 documented in this study (*7*,*75*). The principal clinical manifestations include skin rash, erythema migrans, fever, fatigue, headache, and arthralgia. Most patients recover with effective treatment, and fatal outcomes are rare (*76*).

Babesiosis Babesiosis is a zoonotic parasitic disease caused by *Babesia*, a blood protozoan that infects red blood cells and is transmitted to humans and animals through tick bites (*77*,*78*). Over the past 20 years, more than 100 patients in Zhejiang, Yunnan, Guangxi, and other Chinese PLADs have been infected with *Babesia microti*, suggesting that *B. microti* from field mice may be the primary pathogen causing human babesiosis in China (*79*). Clinical manifestations include fever, headache, myalgia and arthralgia, cutaneous pain or pruritus, lymphadenopathy, abdominal pain, diarrhea or constipation, dyspnea, anemia, and neurological symptoms such as dizziness, nausea, and blurred vision (*80*). While typically mild to moderate in severity, babesiosis can lead to severe outcomes or even death in elderly or immunocompromised patients (*81*).

TBE TBE, also known as forest encephalitis, is an acute infectious disease of the central nervous system caused by the tick-borne encephalitis virus of the genus *Flavivirus*. It is transmitted primarily through the bite of ticks in the genus *Ixodes* (*82*). After entering the body via a tick bite, the virus replicates and migrates to draining lymph nodes before spreading to the bloodstream and crossing the blood-brain barrier, resulting in central nervous system damage (*83*). Between 2007 and 2018, 3,364 cases were reported in Chinese mainland, predominantly in forested areas of northeastern China (*84*). The principal symptoms include fever, headache, myalgia, fatigue, nausea, vomiting, diarrhea, rash, and, in severe cases, neurological manifestations such as altered consciousness, seizures, and paralysis (*85*).

DISCUSSION

Due to China's vast geographical expanse and complex natural environment, combined with the diversity of tick vector species, pathogen types, and intermediate hosts, there likely exist even more types of tick-borne diseases (TBDs) than currently documented. This presents significant challenges for TBD prevention and control efforts in China. Research priorities regarding TBDs in China have evolved over time. Historically, diseases such as Crimean-Congo hemorrhagic fever, African swine fever, Q fever, and Lyme disease were the primary focus (*86*). However, SFTS has received considerable attention in recent years. SFTS is an emerging tick-borne infectious disease first reported in China in 2009 and subsequently identified as a novel bunyavirus in 2010 (*87*). SFTS is particularly lethal, with the elderly patients and those with underlying conditions being susceptible to multiple organ failure following infection (*36*,*88*). Currently, there is no specific antiviral treatment or approved vaccine for SFTSV (*89*). The number of SFTS cases increased gradually in 2020, peaked in 2021, and subsequently decreased each year thereafter. This trend may be attributed to the focus on COVID-19 prevention and control efforts, which diverted attention from SFTS surveillance and management. Additionally, the significant fluctuation in TBD incidence in recent years indicates that monitoring and control measures should be strengthened. The clinical features of TBDs underscore the urgency of addressing these diseases. Furthermore, pathogens of many TBDs, including bacteria and viruses, are transmitted primarily by *H. longicornis*, a tick species widely distributed throughout China (*90*). Recent research has also shown that *Rhipicephalus sanguineus* may serve as a vector for SFTSV (*91*). TBD cases are concentrated in developed agricultural or forestry areas such as Henan, Heilongjiang, and Inner Mongolia. The prevalence of TBDs in these regions is primarily due to favorable environmental factors, including abundant vegetation and livestock resources. These conditions not only provide suitable habitats for the complete tick life cycle from eggs to adults but also promote extensive agropastoral activities within local communities, further exacerbating disease spread (*7*,*92*). These findings suggest that urgent measures are needed to control ticks and tick-borne pathogens.

A limitation of this study is that the literature search was restricted to English-language articles, potentially overlooking studies published in other languages.

CONCLUSION

In summary, due to the rich diversity and widespread distribution of tick species in China, TBDs have become a significant threat to public health. Research on these infections, particularly SFTS, continues to face notable challenges. We urge the use of an integrated One Health approach, at the human-animal-environment interface, to enhance prevention and control measures for TBDs, particularly in regions with developed agriculture and forestry, as well as agropastoral activities.

Conflicts of interest: No conflicts of interest.

doi: 10.46234/ccdcw2025.150

Corresponding authors: Kokouvi Kassegne, ephremk@outmail.fr; Xiaonong Zhou, xiao-nong.zhou@sjtu.edu.cn.

---

[1] School of Global Health, Chinese Centre for Tropical Diseases Research, Shanghai Jiao Tong University School of Medicine, Shanghai, China; [2] School of Public Health, Shanghai Jiao Tong University School of Medicine, Shanghai, China.

Submitted: March 25, 2025
Accepted: June 17, 2025
Issued: June 27, 2025

REFERENCES

1. Boulanger N, Boyer P, Talagrand-Reboul E, Hansmann Y. Ticks and tick-borne diseases. Med Mal Infect 2019;49(2):87 – 97. https://doi.org/10.1016/j.medmal.2019.01.007.
2. Nowak M, Cieniuch S, Stańczak J, Siuda K. Detection of *Anaplasma phagocytophilum* in A*mblyomma flavomaculatum* ticks (Acari: Ixodidae) collected from lizard *Varanus exanthematicus* imported to Poland. Exp Appl Acarol 2010;51(4):363 – 71. https://doi.org/10.1007/s10493-009-9332-5.
3. Cutler SJ, Vayssier-Taussat M, Estrada-Peña A, Potkonjak A, Mihalca AD, Zeller H. Tick-borne diseases and co-infection: current considerations. Ticks Tick Borne Dis 2021;12(1):101607. https://doi.org/10.1016/j.ttbdis.2020.101607.
4. de la Fuente J, Estrada-Peña A, Rafael M, Almazán C, Bermúdez S, Abdelbaset AE, et al. Perception of ticks and tick-borne diseases worldwide. Pathogens 2023;12(10):1258. https://doi.org/10.3390/PATHOGENS12101258.
5. Ogden NH, Lindsay LR. Effects of climate and climate change on vectors and vector-borne diseases: ticks are different. Trends Parasitol 2016;32(8):646 – 56. https://doi.org/10.1016/j.pt.2016.04.015.
6. Ostfeld RS, Brunner JL. Climate change and *Ixodes* tick-borne diseases of humans. Philos Trans Roy Soc B: Biol Sci 2015;370(1665): 20140051. https://doi.org/10.1098/rstb.2014.0051.
7. Zhao GP, Wang YX, Fan ZW, Ji Y, Liu MJ, Zhang WH, et al. Mapping ticks and tick-borne pathogens in China. Nat Commun 2021;12(1):1075. https://doi.org/10.1038/s41467-021-21375-1.
8. Si BY, Jiang T, Zhang Y, Deng YQ, Huo QB, Zheng YC, et al. Complete genome sequence analysis of tick-borne encephalitis viruses isolated in northeastern China. Arch Virol 2011;156(8):1485 – 8. https://doi.org/10.1007/s00705-011-1031-y.
9. Xu BL, Liu LC, Huang XY, Ma H, Zhang Y, Du YH, et al. Metagenomic analysis of fever, thrombocytopenia and leukopenia syndrome (FTLS) in Henan Province, China: discovery of a new bunyavirus. PLoS Pathog 2011;7(11):e1002369. https://doi.org/10.1371/journal.ppat.1002369.
10. Yu XJ, Liang MF, Zhang SY, Liu Y, Li JD, Sun YL, et al. Fever with thrombocytopenia associated with a novel bunyavirus in China. N Engl J Med 2011;364(16):1523 – 32. https://doi.org/10.1056/NEJMoa1010095.
11. Zhang YZ, Zhou DJ, Xiong YW, Chen XP, He YW, Sun QZ, et al. Hemorrhagic fever caused by a novel tick-borne *Bunyavirus* in Huaiyangshan, China. Chin J Epidemiol 2011;32(3):209 – 20. https://doi.org/10.3760/cma.j.issn.0254-6450.2011.03.001.
12. Kang XP, Li YC, Wei JJ, Zhang Y, Bian C, Wang K, et al. Elevation of matrix metalloproteinase-9 level in cerebrospinal fluid of tick-borne encephalitis patients is associated with IgG extravassation and disease severity. PLoS One 2013;8(11):e77427. https://doi.org/10.1371/journal.pone.0077427.
13. Lam TTY, Liu W, Bowden TA, Cui N, Zhuang L, Liu K, et al. Evolutionary and molecular analysis of the emergent severe fever with thrombocytopenia syndrome virus. Epidemics 2013;5(1):1 – 10. https://doi.org/10.1016/j.epidem.2012.09.002.
14. Ding F, Guan XH, Kang K, Ding SJ, Huang LY, Xing XS, et al. Risk factors for bunyavirus-associated severe fever with thrombocytopenia syndrome, China. PLoS Negl Trop Dis 2014;8(10):e3267. https://doi.org/10.1371/journal.pntd.0003267.
15. Ding SJ, Niu GY, Xu XH, Li JP, Zhang XM, Yin HY, et al. Age is a critical risk factor for severe fever with thrombocytopenia syndrome. PLoS One 2014;9(11):e111736. https://doi.org/10.1371/journal.pone.0111736.
16. Liu K, Cui N, Fang LQ, Wang BJ, Lu QB, Peng W, et al. Epidemiologic features and environmental risk factors of severe fever with thrombocytopenia syndrome, Xinyang, China. PLoS Negl Trop Dis 2014;8(5):e2820. https://doi.org/10.1371/journal.pntd.0002820.
17. Xing XS, Guan XH, Liu L, Zhan JB, Jiang HB, Liu L, et al. Natural transmission model for severe fever with thrombocytopenia syndrome bunyavirus in villages of Hubei Province, China. Medicine 2016;95(4): e2533. https://doi.org/10.1097/MD.0000000000002533.
18. Huang DY, Jiang YP, Liu XP, Wang B, Shi JM, Su Z, et al. A cluster of symptomatic and asymptomatic infections of severe fever with thrombocytopenia syndrome caused by person-to-person transmission. Am J Trop Med Hyg 2017;97(2):396 – 402. https://doi.org/10.4269/ajtmh.17-0059.
19. Li ZF, Hu JL, Cui LB, Hong Y, Liu JW, Li PF, et al. Increased prevalence of severe fever with thrombocytopenia syndrome in Eastern China clustered with multiple genotypes and reasserted virus during 2010-2015. Sci Rep 2017;7(1):6503. https://doi.org/10.1038/s41598-017-06853-1.
20. Wu YY, Fu GM, Guo S, Ye L, Hou J, Wang JN, et al. The effects of health education and promotion with regard to severe fever with thrombocytopenia syndrome (SFTS) in rural residents: a pilot study in China. Biosci Trends 2018;11(6):697 – 701. https://doi.org/10.5582/bst.2017.01252.
21. Xing XS, Guan XH, Liu L, Xu JQ, Li GM, Zhan JB, et al. A case-control study of risk sources for severe fever with thrombocytopenia syndrome in Hubei Province, China. Int J Infect Dis 2017;55:86 – 91. https://doi.org/10.1016/j.ijid.2017.01.003.
22. Jia B, Wu WH, Huang R, Wang GY, Song PX, Li Y, et al. Characterization of clinical features and outcome for human-to-human

transmitted severe fever with thrombocytopenia syndrome. Infect Dis 2018;50(8):601 – 8. https://doi.org/10.1080/23744235.2018.1449962.

23. Xu HH, Wei YY, Ma HQ, Liu YY, Zhang YL, Hu LF, et al. Alterations of gut microbiome in the patients with severe fever with thrombocytopenia syndrome. Front Microbiol 2018;9:2315. https://doi.org/10.3389/fmicb.2018.02315.
24. Hu JL, Li ZF, Cai JP, Liu DL, Zhang XF, Jiang RJ, et al. A cluster of bunyavirus-associated severe fever with thrombocytopenia syndrome cases in a coastal plain area in China, 2015: identification of a previously unidentified endemic region for severe fever with thrombocytopenia bunyavirus. Open Forum Infect Dis 2019;6(6): ofz209. https://doi.org/10.1093/ofid/ofz209.
25. Jia N, Liu HB, Ni XB, Bell-Sakyi L, Zheng YC, Song JL, et al. Emergence of human infection with Jingmen tick virus in China: a retrospective study. eBioMedicine 2019;43:317 – 24. https://doi.org/10.1016/j.ebiom.2019.04.004.
26. Qi R, Qin XR, Wang L, Han HJ, Cui F, Yu H, et al. Severe fever with thrombocytopenia syndrome can masquerade as hemorrhagic fever with renal syndrome. PLoS Negl Trop Dis 2019;13(3):e0007308. https://doi.org/10.1371/journal.pntd.0007308.
27. Tian B, Qu D, Sasaki A, Chen JY, Deng BC. Acute pancreatitis in patients with severe fever with thrombocytopenia syndrome virus infection. Pancreatology 2020;20(8):1631 – 6. https://doi.org/10.1016/j.pan.2020.09.024.
28. Zhang YY, Liu DX, Fan WB, Yu JH, Liu L, Du WJ, et al. Hazardous alcohol consumption and aging synergistically increase the risk of death in patients with severe fever with thrombocytopenia syndrome. Ticks Tick Borne Dis 2020;11(6):101505. https://doi.org/10.1016/j.ttbdis.2020.101505.
29. Du YD, Mi ZH, Xie YP, Lu DS, Zheng HJ, Sun H, et al. Insights into the molecular basis of tick-borne encephalitis from multiplatform metabolomics. PLoS Negl Trop Dis 2021;15(3):e0009172. https://doi.org/10.1371/journal.pntd.0009172.
30. Hu LF, Kong QX, Liu YY, Li JJ, Bian TT, Ma XJ, et al. Time course of severe fever with thrombocytopenia syndrome virus and antibodies in patients by long-term follow-up study, China. Front Microbiol 2021;12:744037. https://doi.org/10.3389/fmicb.2021.744037.
31. Wang YC, Wei ZK, Lv XL, Han SZ, Wang ZD, Fan CF, et al. A new nairo-like virus associated with human febrile illness in China. Emerg Microbes Infect 2021;10(1):1200 – 8. https://doi.org/10.1080/22221751.2021.1936197.
32. You EQ, Wang L, Zhang L, Wu JJ, Zhao KF, Huang F. Epidemiological characteristics of severe fever with thrombocytopenia syndrome in Hefei of Anhui Province: a population-based surveillance study from 2011 to 2018. Eur J Clin Microbiol Infect Dis 2021;40(5): 929 – 39. https://doi.org/10.1007/s10096-020-04098-x.
33. Zhao J, Lu QB, Li H, Yuan Y, Cui N, Yuan C, et al. Sex differences in case fatality rate of patients with severe fever with thrombocytopenia syndrome. Front Microbiol 2021;12:738808. https://doi.org/10.3389/fmicb.2021.738808.
34. Dai ZN, Peng XF, Li JC, Zhao J, Wu YX, Yang X, et al. Effect of genomic variations in severe fever with thrombocytopenia syndrome virus on the disease lethality. Emerg Microbes Infect 2022;11(1):1672 – 82. https://doi.org/10.1080/22221751.2022.2081617.
35. Han XH, Ma Y, Liu HY, Li D, Wang Y, Jiang FH, et al. Identification of severe fever with thrombocytopenia syndrome virus genotypes in patients and ticks in Liaoning Province, China. Parasit Vectors 2022;15(1):120. https://doi.org/10.1186/s13071-022-05237-3.
36. Zhao J, Ge HH, Wang G, Lin L, Yuan Y, Xu YL, et al. Fatal patients with severe fever with thrombocytopenia syndrome in China. Int J Infect Dis 2022;125:10 – 6. https://doi.org/10.1016/j.ijid.2022.10.008.
37. Liu T, Zhang NN, Li HW, Hou ST, Liu XW. Analysis of severe fever with thrombocytopenia syndrome cluster in East China. Virol J 2023;20(1):199. https://doi.org/10.1186/s12985-023-02155-3.
38. Ren YT, Tian HP, Xu JL, Liu MQ, Cai K, Chen SL, et al. Extensive genetic diversity of severe fever with thrombocytopenia syndrome virus circulating in Hubei Province, China, 2018-2022. PLoS Negl Trop Dis 2023;17(9):e0011654. https://doi.org/10.1371/journal.pntd.0011654.
39. Zheng HX, Geng Y, Gu CG, Li M, Mao MX, Wan YW, et al. A reservoir computing with boosted topology model to predict encephalitis and mortality for patients with severe fever with thrombocytopenia syndrome: a retrospective multicenter study. Infect Dis Ther 2023;12(5):1379 – 91. https://doi.org/10.1007/s40121-023-00808-y.
40. Fei X, Feng BB, Fang K, Ren WH. Risk factors for mortality in severe fever with thrombocytopenia syndrome patients with central nervous system complications. Med Sci Monit 2023;29:e938427. https://doi.org/10.12659/MSM.938427.
41. Lv XL, Liu ZY, Li L, Xu WB, Yuan YX, Liang XJ, et al. Yezo virus infection in tick-bitten patient and ticks, northeastern China. Emerg Infect Dis 2023;29(4):797 – 800. https://doi.org/10.3201/eid2904.220885.
42. Li HY, Zhou Y, Wang WJ, Guo DM, Huang S, Jie SH. The clinical characteristics and outcomes of patients with human granulocytic anaplasmosis in China. Int J Infect Dis 2011;15(12):e859 – 66. https://doi.org/10.1016/j.ijid.2011.09.008.
43. Zhang LJ, Cui F, Wang LL, Zhang LL, Zhang JS, Wang SW, et al. Investigation of anaplasmosis in Yiyuan County, Shandong Province, China. Asian Pac J Trop Med 2011;4(7):568 – 72. https://doi.org/10.1016/S1995-7645(11)60148-X.
44. Wang Y, Chen CF, Zhang LJ. Molecular characterization of *msp2/p44* of *Anaplasma phagocytophilum* isolated from infected patients and *Haemaphysalis longicorni*s in Laizhou Bay, Shandong Province, China. PLoS One 2013;8(10):e78189. https://doi.org/10.1371/journal.pone.0078189.
45. Zhang LJ, Wang GQ, Liu QH, Chen CF, Li J, Long B, et al. Molecular analysis of *Anaplasma phagocytophilum* isolated from patients with febrile diseases of unknown etiology in China. PLoS One 2013;8(2): e57155. https://doi.org/10.1371/journal.pone.0057155.
46. Ni XB, Jia N, Jiang BG, Sun T, Zheng YC, Huo QB, et al. Lyme borreliosis caused by diverse genospecies of *Borrelia burgdorferi* sensu lato in northeastern China. Clin Microbiol Infect 2014;20(8):808 – 14. https://doi.org/10.1111/1469-0691.12532.
47. Jiao XY, Fan ZC, Li YZ, Tang YT, Ke CW. Clinical and laboratory features parameters of human granulocytic anaplasmosis (HGA) in patients admitted to hospital in Guangdong Province, China. Trop Doct 2015;45(4):209 – 13. https://doi.org/10.1177/0049475515579772.
48. Li H, Zheng YC, Ma L, Jia N, Jiang BG, Jiang RR, et al. Human infection with a novel tick-borne *Anaplasma* species in China: a surveillance study. Lancet Infect Dis 2015;15(6):663 – 70. https://doi.org/10.1016/S1473-3099(15)70051-4.
49. Li H, Cui XM, Cui N, Yang ZD, Hu JG, Fan YD, et al. Human infection with novel spotted fever group rickettsia genotype, China, 2015. Emerg Infect Dis 2016;22(12):2153 – 6. https://doi.org/10.3201/eid2212.160962.
50. Liu W, Li H, Lu QB, Cui N, Yang ZD, Hu JG, et al. *Candidatus* rickettsia tarasevichiae infection in eastern central China: a case series. Ann Intern Med 2016;164(10):641 – 8. https://doi.org/10.7326/M15-2572.
51. Jiang BG, Jia N, Jiang JF, Zheng YC, Chu YL, Jiang RR, et al. *Borrelia miyamotoi* infections in humans and ticks, northeastern China. Emerg Infect Dis 2018;24(2):236 – 41. https://doi.org/10.3201/eid2402.160378.
52. Li H, Zhang PH, Huang Y, Du J, Cui N, Yang ZD, et al. Isolation and identification of *Rickettsia raoultii* in human cases: a surveillance study in 3 medical centers in China. Clin Infect Dis 2018;66(7):1109 – 15. https://doi.org/10.1093/cid/cix917.
53. Lu QY, Yu JP, Yu LQ, Zhang YJ, Chen YT, Lin MA, et al. *Rickettsia japonica* infections in humans, Zhejiang Province, China, 2015. Emerg Infect Dis 2018;24(11):2077 – 9. https://doi.org/10.3201/eid2411.170044.
54. Gaowa, Wulantuya, Yin XH, Guo SC, Ding CL, Cao MZ, et al. Spotted fever group rickettsiae in Inner Mongolia, China, 2015-2016. Emerg Infect Dis 2018;24(11):2105 – 7. https://doi.org/10.3201/eid2411.162094.

55. Li H, Zhang PH, Du J, Yang ZD, Cui N, Xing B, et al. *Rickettsia japonica* infections in humans, Xinyang, China, 2014-2017. Emerg Infect Dis 2019;25(9):1719 – 22. https://doi.org/10.3201/eid2509.171421.
56. Wang F, Ma MB, Luo SY, Yan M, Tao LY, Liu AH, et al. Seroprevalence of tick-borne *Anaplasma phagocytophilum* infection in healthy adult population and patients with acute undifferentiated fever from the Yunnan Province of China. Vector Borne Zoonotic Dis 2019;19(8):576 – 81. https://doi.org/10.1089/vbz.2018.2389.
57. Jia N, Liu HB, Zheng YC, Shi WQ, Wei R, Chu YL, et al. Cutaneous immunoprofiles of three spotted fever group rickettsia cases. Infect Immun 2020;88(4):e00686 – 19. https://doi.org/10.1128/IAI.00686-19.
58. Li H, Li XM, Du J, Zhang XA, Cui N, Yang ZD, et al. *Candidatus* rickettsia xinyangensis as cause of spotted fever group rickettsiosis, Xinyang, China, 2015. Emerg Infect Dis 2020;26(5):985 – 8. https://doi.org/10.3201/eid2605.170294.
59. Gao Y, Lv XL, Han SZ, Wang W, Liu Q, Song MX. First detection of *Borrelia miyamotoi* infections in ticks and humans from the northeast of Inner Mongolia, China. Acta Trop 2021;217:105857. https://doi.org/10.1016/j.actatropica.2021.105857.
60. Lyu Y, Shen Y, Hu CY, Xu PP, Qin W, Gong L, et al. The first reported outbreak of an undetermined species of human infection with spotted fever group Rickettsia in Lu'an, China. Acta Trop 2021;223:106072. https://doi.org/10.1016/j.actatropica.2021.106072.
61. Jiang JF, Zheng YC, Jiang RR, Li H, Huo QB, Jiang BG, et al. Epidemiological, clinical, and laboratory characteristics of 48 cases of "*Babesia venatorum*" infection in China: a descriptive study. Lancet Infect Dis 2015;15(2):196 – 203. https://doi.org/10.1016/S1473-3099(14)71046-1.
62. Jia N, Zheng YC, Jiang JF, Jiang RR, Jiang BG, Wei R, et al. Human babesiosis caused by a *Babesia* Crassa-like pathogen: a case series. Clin Infect Dis 2018;67(7):1110 – 9. https://doi.org/10.1093/cid/ciy212.
63. Wang JM, Zhang SD, Yang JQ, Liu JL, Zhang DK, Li YQ, et al. *Babesia divergens* in human in Gansu province, China. Emerg Microbes Infect 2019;8(1):959 – 61. https://doi.org/10.1080/22221751.2019.1635431.
64. Zhao L, Jiang RR, Jia N, Ning NZ, Zheng YC, Huo QB, et al. Human case infected with *Babesia venatorum*: a 5-year follow-up study. Open Forum Infect Dis 2020;7(3):ofaa062. https://doi.org/10.1093/ofid/ofaa062.
65. Li J, Li S, Yang L, Cao PF, Lu JH. Severe fever with thrombocytopenia syndrome virus: a highly lethal bunyavirus. Crit Rev Microbiol 2021;47(1):112 – 25. https://doi.org/10.1080/1040841X.2020.1847037.
66. Liu Q, He B, Huang SY, Wei F, Zhu XQ. Severe fever with thrombocytopenia syndrome, an emerging tick-borne zoonosis. Lancet Infect Dis 2014;14(8):763 – 72. https://doi.org/10.1016/S1473-3099(14)70718-2.
67. Robinson MT, Satjanadumrong J, Hughes T, Stenos J, Blacksell SD. Diagnosis of spotted fever group *Rickettsia* infections: the Asian perspective. Epidemiol Infect 2019;147:e286. https://doi.org/10.1017/S0950268819001390.
68. Parola P, Paddock CD, Socolovschi C, Labruna MB, Mediannikov O, Kernif T, et al. Update on tick-borne rickettsioses around the world: a geographic approach. Clin Microbiol Rev 2013;26(4):657 – 702. https://doi.org/10.1128/CMR.00032-13.
69. MacQueen D, Centellas F. Human granulocytic anaplasmosis. Infect Dis Clin North Am 2022;36(3):639 – 54. https://doi.org/10.1016/j.idc.2022.02.008.
70. Dumic I, Jevtic D, Veselinovic M, Nordstrom CW, Jovanovic M, Mogulla V, et al. Human granulocytic anaplasmosis-a systematic review of published cases. Microorganisms 2022;10(7):1433. https://doi.org/10.3390/MICROORGANISMS10071433.
71. Jin HT, Wei F, Liu Q, Qian J. Epidemiology and control of human granulocytic anaplasmosis: a systematic review. Vector Borne Zoonotic Dis 2012;12(4):269 – 74. https://doi.org/10.1089/vbz.2011.0753.
72. Zhang SY, Hai R, Li WY, Li GH, Lin GY, He JR, et al. Seroprevalence of human granulocytotropic anaplasmosis in central and southeastern China. Am J Trop Med Hyg 2009;81(2):293 – 5. https://doi.org/10.4269/ajtmh.2009.81.293.
73. Hamburg BJ, Storch GA, Micek ST, Kollef MH. The importance of early treatment with doxycycline in human ehrlichiosis. Medicine 2008;87(2):53 – 60. https://doi.org/10.1097/MD.0b013e318168da1d.
74. Wu XB, Na RH, Wei SS, Zhu JS, Peng HJ. Distribution of tick-borne diseases in China. Parasit Vectors 2013;6:119. https://doi.org/10.1186/1756-3305-6-119.
75. Mead PS. Epidemiology of Lyme disease. Infect Dis Clin North Am 2015;29(2):187 – 210. https://doi.org/10.1016/j.idc.2015.02.010.
76. Stanek G, Strle F. Lyme borreliosis-from tick bite to diagnosis and treatment. FEMS Microbiol Rev 2018;42(3):233 – 58. https://doi.org/10.1093/femsre/fux047.
77. Vannier E, Krause PJ. Human babesiosis. N Engl J Med 2012;366(25):2397 – 407. https://doi.org/10.1056/NEJMra1202018.
78. Gray JS, Estrada-Peña A, Zintl A. Vectors of babesiosis. Annu Rev Entomol 2019;64:149 – 65. https://doi.org/10.1146/annurev-ento-011118-111932.
79. Chen ZT, Li HQ, Gao XG, Bian AN, Yan HR, Kong DL, et al. Human Babesiosis in China: a systematic review. Parasitol Res 2019;118(4):1103 – 12. https://doi.org/10.1007/s00436-019-06250-9.
80. Voisin O, Monpierre L, Le Lorc'h E, Pilmis B, Le Monnier A, Mourad JJ, et al. A typical babesiosis in an immunocompetent patient. Ann Biol Clin (Paris) 2021;79(5):456 – 9. https://doi.org/10.1684/abc.2021.1675.
81. Stein E, Elbadawi LI, Kazmierczak J, Davis JP. Babesiosis surveillance - Wisconsin, 2001-2015. MMWR Morb Mortal Wkly Rep 2017;66(26):687 – 91. https://doi.org/10.15585/mmwr.mm6626a2.
82. Phipps LP, Johnson N. Tick-borne encephalitis virus. J Med Microbiol 2022;71(5):001492. https://doi.org/10.1099/jmm.0.001492.
83. Johnson N, Migné CV, Gonzalez G. Tick-borne encephalitis. Curr Opin Infect Dis 2023;36(3):198 – 202. https://doi.org/10.1097/QCO.0000000000000924.
84. Chen XJ, Li F, Yin QK, Liu WJ, Fu SH, He Y, et al. Epidemiology of tick-borne encephalitis in China, 2007- 2018. PLoS One 2019;14(12):e0226712. https://doi.org/10.1371/journal.pone.0226712.
85. Chiffi G, Grandgirard D, Leib SL, Chrdle A, Růžek D. Tick-borne encephalitis: a comprehensive review of the epidemiology, virology, and clinical picture. Rev Med Virol 2023;33(5):e2470. https://doi.org/10.1002/rmv.2470.
86. Luan YX, Gou JM, Zhong DJ, Ma L, Yin CS, Shu MF, et al. The tick-borne pathogens: an overview of China's situation. Acta Parasitol 2023;68(1):1 – 20. https://doi.org/10.1007/s11686-023-00658-1.
87. Madison-Antenucci S, Kramer LD, Gebhardt LL, Kauffman E. Emerging tick-borne diseases. Clin Microbiol Rev 2020;33(2):e00083 – 18. https://doi.org/10.1128/CMR.00083-18.
88. Seo JW, Kim D, Yun N, Kim DM. Clinical update of severe fever with thrombocytopenia syndrome. Viruses 2021;13(7):1213. https://doi.org/10.3390/v13071213.
89. Kim D, Lai CJ, Cha I, Jung JU. Current progress of severe fever with thrombocytopenia syndrome virus (SFTSV) vaccine development. Viruses 2024;16(1):128. https://doi.org/10.3390/V16010128.
90. Cun DJ, Wang Q, Yao XY, Ma B, Zhang Y, Li LH. Potential suitable habitats of *Haemaphysalis longicornis* in China under different climatic patterns. Chin J Schistosomiasis Control 2021;33(4):359 – 64. https://doi.org/10.16250/j.32.1374.2021023.
91. Yuan CF, Lu YJ, Li JQ, Chen C, Wang YH, Zheng AH, et al. Infection and transovarial transmission of severe fever with thrombocytopenia syndrome virus in *Rhipicephalus sanguineus* in Hainan Island, China. Integr Zool 2023;18(6):1009 – 13. https://doi.org/10.1111/1749-4877.12716.
92. Fei SW, Zhao HQ, Yin JX, Wang L, Sun ZS, Zhang WG, et al. Molecular identification and genetic characterization of public health threatening ticks - Chongming Island, China, 2021-2022. China CDC Wkly 2023;5(37):815 – 21. https://doi.org/10.46234/ccdcw2023.156.

Youth Editorial Board

Indexed by Science Citation Index Expanded (SCIE), Social Sciences Citation Index (SSCI), PubMed Central (PMC), Scopus, Chinese Scientific and Technical Papers and Citations, and Chinese Science Citation Database (CSCD)

The inauguration of *China CDC Weekly* is in part supported by Project for Enhancing International Impact of China STM Journals Category D (PIIJ2-D-04-(2018)) of China Association for Science and Technology (CAST).

CCDC weekly

Vol. 7 No. 26 Jun. 27, 2025

Responsible Authority

National Disease Control and Prevention Administration

Sponsor

Chinese Center for Disease Control and Prevention

Editing and Publishing

China CDC Weekly Editorial Office
No.155 Changbai Road, Changping District, Beijing, China
Tel: 86-10-63150501, 63150701
Email: weekly@chinacdc.cn

CSSN

ISSN 2096-7071 (Print)
ISSN 2096-3101 (Online)
CN 10-1629/R1